Inflamm. Res. (2011) 60:879–888
DOI 10.1007/s00011-011-0348-z

Inflammation Research

ORIGINAL RESEARCH PAPER

Inhibition of macrophage activation and suppression of graft rejection by DTCM-glutarimide, a novel piperidine derived from the antibiotic 9-methylstreptimidone

Masatoshi Takeiri · Miyuki Tachibana · Ayumi Kaneda · Ayumi Ito · Yuichi Ishikawa · Shigeru Nishiyama · Ryoichi Goto · Kenichiro Yamashita · Susumu Shibasaki · Gentaro Hirokata · Michitaka Ozaki · Satoru Todo · Kazuo Umezawa

Received: 14 November 2010 / Revised: 15 April 2011 / Accepted: 13 May 2011 / Published online: 28 May 2011

Abstract
Objective We have previously synthesized a novel piperidine compound, 3-[(dodecylthiocarbonyl)methyl] glutarimide (DTCM-glutarimide), that inhibits LPS-induced NO production, and in the present research we studied further the anti-inflammatory activity of DTCM-glutarimide in a macrophage cell line and in mice bearing transplanted hearts.
Materials and methods Mouse macrophage-like RAW264.7 cells were employed for the evaluation of cellular inflammatory activity. DTCM-glutarimide was synthesized in our laboratory. The AP-1 activity was measured by nuclear translocation and phosphorylation. For the heart transplantation experiment, male C57BL/6 (H-2b) and BALB/c (H-2d) mice were used as donor and recipient, respectively. DTCM-glutarimide was administered intraperitoneally.
Results DTCM-glutarimide inhibited the LPS-induced expression of iNOS and COX-2 in macrophages; but, unexpectedly, it did not inhibit LPS-induced NF-κB activation. Instead, it inhibited the nuclear translocation of both c-Jun and c-Fos. It also inhibited LPS-induced c-Jun phosphorylation. Moreover, it inhibited the mixed lymphocyte reaction in primary cultures of mouse spleen cells; and furthermore, in mice it prolonged the graft survival in heart transplantation experiments.
Conclusion The novel piperidine compound, DTCM-glutarimide, was found to be a new inhibitor of macrophage activation, inhibiting AP-1 activity. It also inhibited graft rejection in mice, and thus may be a candidate for an anti-inflammatory agent.

Keywords DTCM-glutarimide · LPS · AP-1 · Mixed lymphocyte reaction · Heart transplantation

Responsible Editor: Graham Wallace.

M. Takeiri · M. Tachibana · A. Kaneda · A. Ito · Y. Ishikawa · S. Nishiyama · K. Umezawa (✉)
Center for Chemical Biology, School of Fundamental Science and Technology, Faculty of Science and Technology, Keio University, 3-14-1 Hiyoshi, Kohoku-ku, Yokohama 223-0061, Japan
e-mail: umezawa@applc.keio.ac.jp

R. Goto · K. Yamashita · S. Shibasaki · G. Hirokata · M. Ozaki · S. Todo
Department of Surgery, Hokkaido University School of Medicine, Sapporo 060-8683, Japan

Introduction

Microbial and plant-derived bioactive metabolites are a treasure-trove of organic compounds having various structures and biological activities. Molecular designing of these bioactive metabolites often provides further active and useful compounds. We have previously designed dehydroxymethylepoxyquinomicin (DHMEQ) based on the structure of epoxyquinomicins, which are weak antibiotics isolated from *Amicolatopsis* [1, 2]. DHMEQ inhibits NF-κB by direct binding to NF-κB components including p65, p50, RelB, and cRel [3], and it shows potent anti-inflammatory and anticancer effects in animal experiments [4–6]. It also prolongs the graft survival in mouse heart transplantation experiments [7]. Since DHMEQ was effective in suppression of many disease models, further screening for NF-κB inhibitors was carried out in which NF-κB activity was monitored in terms of lipopolysaccharide (LPS)-induced NO production in macrophages. Thereby, we isolated 9-methylstreptimidone, a known piperidine compound (Fig. 1), from *Streptomyces* and

found this NF-κB inhibitor selectively induces apoptosis in adult T-cell leukemia cells in which NF-κB is excessively activated [8]. Since the production of 9-methylstreptimidone by the producing organism is poor, we synthesized a number of its derivatives. Among them, we found 3-[(dodecylthiocarbonyl)methyl]glutarimide (DTCM-glutarimide, Fig. 1) to inhibit LPS-induced NO production strongly in mouse macrophage RAW264.7 cells [9].

In the present research we studied further the anti-inflammatory activity of DTCM-glutarimide in a macrophage cell line. This analog inhibited the expression of iNOS and COX-2, possibly due to the inhibition of AP-1 activation. It also showed anti-inflammatory activity in a transplantation experiment.

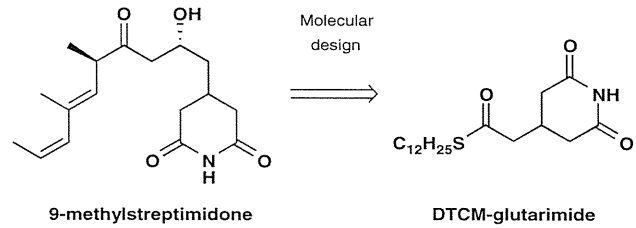

Fig. 1 Structures of 9-methylstreptimidone and DTCM-glutarimide

Materials and methods

Materials

DTCM-glutarimide (3-[(dodecylthiocarbonyl)methyl]glutarimide) was synthesized by us as described earlier [9]. Mouse monoclonal anti-COX-2 antibody was purchased from BD Bioscience Pharmingen, Franklin Lakes, NJ, USA. Mouse monoclonal anti-NOS2, anti-ERK1, and anti-p65 NF-κB and rabbit polyclonal anti-p38, anti-JNK, and anti-c-Fos antibodies were obtained from Santa Cruz Biotechnology, CA, USA. Rabbit polyclonal anti-phospho-p38, anti-phospho-p44/42 MAP kinase, anti-phospho-JNK, and anti-lamin A/C, as well as rabbit monoclonal anti-c-Jun and anti-phospho-c-Jun antibodies, were purchased from Cell Signaling Technology, Beverly, MO, USA. Anti-rabbit-IgG antibody derived from goat and anti-mouse-IgG antibody derived from sheep were purchased from GE Healthcare, Little Chalfont, UK. Anti-α-tubulin antibody was purchased from Sigma-Aldrich, St. Louis, MO, USA.

Cell culture

Mouse macrophage RAW264.7 cells were grown in Dulbecco's modified Eagle's medium (DMEM; Nissui, Tokyo, Japan) supplemented with 10% fetal bovine serum (JRH Biosciences, Lenexa, KS, USA), 200 μg/ml kanamycin (Sigma, St. Louis, MO, USA), 100 units/ml penicillin G (Sigma), 600 μg/ml L-glutamine (Sigma), and 2.25 g/L $NaHCO_3$ at 37°C under 5% CO_2 plus air.

NO production assay

Cells in complete medium (1×10^5 cells/ml) were seeded in a 96-well plate (Corning Inc., Corning, NY, USA), with each well receiving 100 μl of the cell suspension. On the next day, the cells were treated with DTCM-glutarimide for 2 h and then stimulated with 3 μg/ml LPS for 20 h. Then 100 μl Griess reagent solution was added to each well [21]. The concentration of NO was obtained by measuring the absorbance at 570 nm with a microplate reader.

MTT assay

Cells in complete medium (1×10^5 cells/ml) were seeded in a 96-well plate, with each well receiving 100 μl of the cell suspension. On the next day, the cells were treated with DTCM-glutarimide for 2 h and then stimulated with 3 μg/ml LPS for 20 h. Then, 10 μl of MTT (3-[4,5-dimethylthiazol-2–yl]-2,5-diphenyltetrazoliumbromide) solution was added to each well, and the cells were incubated for 4 h at 37°C under 5% CO_2 plus air. Subsequently, the culture supernatant was replaced with 100 μl DMSO to dissolve the formazan crystals made from MTT by the enzymatic action of succinic dehydrogenase in the mitochondria of live cells. The absorbance at 570 nm was measured with a microplate reader.

Western blotting

Cells in complete medium (1×10^5 or 3×10^5 cells/ml) were seeded into 60-mm dishes (Corning). On the next day, the cells were treated with DTCM-glutarimide for 2 h and then stimulated with 3 μg/ml LPS for the desired times. Then the cells were lysed with lysis buffer (20 mM Tris [pH 8.0], 150 mM NaCl, 2 mM EDTA, 100 mM NaF, 400 μM Na_3VO_4, 1% Nonidet P-40, 1 μg/ml leupeptin, 1 μg/ml aprotinin, and 1 mM PMSF). Total cell extracts or nuclear extracts (about 10–30 μg of protein) were boiled in Laemmli loading buffer and subjected to SDS-polyacrylamide gel electrophoresis. Proteins were transferred at 200 mA for 1 h onto Hybond-P membranes (GE Healthcare, Little Chalfont, UK). The membranes were incubated for 30 min at room temperature (RT) for blocking in Tris-buffered saline with Tween 20 (TBST), composed of 10 mM Tris–HCl, pH 8.0, containing 150 mM NaCl, 0.1% Tween 20 (v/v), and 5% (w/v) nonfat dry milk. After

having been washed for 1 h in TBST, the membrane was incubated for 1 h at RT in a 1:3,000 dilution of a primary antibody in TBST. After a 1 h wash in TBST, the membrane was next incubated for 1 h at RT with anti-IgG rabbit or anti-IgG mouse antibody (diluted at 1:3,000 in TBST) linked to horseradish peroxidase. After having been washed for 1 h in TBST, immunoreactive proteins were visualized by use of an ECL detection system, Immobilon Western (Millipore, Billerica, MA, USA). Exposure to RX-U films (Fuji Film, Kanagawa, Japan) was carried out for 10 s to 10 min.

RT-PCR

Cells in complete medium (1×10^5 cells/ml) were seeded into 60-mm dishes (Corning). On the next day, the cells were treated with DTCM-glutarimide for 2 h and then stimulated with 3 μg/ml LPS for the desired times. Total cellular mRNAs were extracted from cells using Trizol reagent (Invitrogen, Carlsbad, CA, USA), then 1 μg of mRNA was converted to cDNA using High-Capacity cDNA Reverse Transcription Kits (Life Technology, Carlsbad, CA, USA), and 2 μl of the cDNA mixture was used for enzymatic amplification using TaKaRa Taq™ (Takara Bio, Shiga, Japan). The primer sequences were 5′-TTTGACCAGAGGACCCAGAG and 5′-ATGGCCG ACCTGATGTTGCC (for iNOS), 5′-AGAAGGAAATGG CTGCAGAA and 5′-GCTCGGCTTCCAGTATTGAG (for COX-2), 5′-CTTCGAGCACGAGATGGCCA and 5′-CC AGACAGCACTGTGTTGGC (for β-actin).

Enzyme-linked immunosorbent assay

Cells in complete medium (4×10^5 cells/ml) were seeded into a 48-well plate (Corning), with each well receiving 500 μl of the cell suspension. On the next day, the cells were treated with DTCM-glutarimide for 2 h and then stimulated with 3 μg/ml LPS for 20 h. The cell-free medium was collected into a 1.5 ml tube and stored at −80°C prior to the assay. The concentration of IL-6 was quantified by using a commercially available sandwich-type enzyme-linked immunosorbent assay (ELISA) kit specific for murine IL-6 (Techne, Minneapolis, MN, USA). After the wells had been coated with the specific antibodies, 2 h later they were washed with wash buffer; then the thawed medium was added to the assay wells. Next, the appropriate horseradish peroxidase-conjugated polyclonal antibody against IL-6 was added, and the plate was incubated for 2 h at RT. After the wells had been washed with Ca^{2+}, Mg^{2+}-free PBS (PBS^-)—Tween, the substrate solution was added to the wells. The color reaction was stopped by the addition of sulfuric acid, and the intensity was expressed by absorbance (A450–A570) read with a microplate reader. The standard curve for IL-6 protein was prepared as indicated by the manufacturer, and the protein level in the sample was calculated from this standard curve.

Immunofluorescence

Cells in complete medium (1×10^6 cells/ml) were seeded onto glass coverslips in a 12-well plate (Corning). On the next day, the cells were treated with DTCM-glutarimide for 2 h and then stimulated with 3 μg/ml LPS for 30 min. Next, the cells were fixed for 10 min with 3% paraformaldehyde in PBS^-, washed 2 times with PBS^-, and permeabilized for 5 min with 1% Triton X in PBS^-. After having been washed again 2 times with PBS^-, the cells were incubated with 10% normal blocking serum in 500 μl of PBS^- for 20 min at RT and washed three times with PBS^-. Then, they were stained with anti-p65, anti-c-Fos antibody (Santa Cruz Biotechnology, California, USA) or anti-c-Jun antibody (Cell Signaling Technology, Beverly, MA, USA) for 45 min at RT, washed 3 times with PBS^-, and stained with anti-rabbit-FITC secondary antibody (Molecular Probes, Reiden, The Netherlands) for 1 h at RT. After three final washings with PBS^-, the cells were photographed through B2 and UV filters at a magnification of 400× with a camera attached to a confocal microscope.

Nuclear protein extraction

Nuclear extracts were prepared according to the method described before [10]. Cells (3×10^5 cells/ml) were grown in 60-mm dishes (Corning) and incubated with the desired chemicals. They were then harvested and washed with phosphate-buffered saline (PBS), suspended in 400 μl of buffer A (10 mM HEPES [pH 7.8], 10 mM KCl, 2 mM $MgCl_2$, 0.1 mM EDTA, 1 mM DTT, 0.1 mM PMSF), and incubated on ice for 15 min. Nuclei were pelleted by centrifugation for 5 min at 14,000 rpm, resuspended in 20–40 μl of buffer C (50 mM HEPES [pH 7.8], 50 mM KCl, 300 mM NaCl, 0.1 mM EDTA, 1 mM DTT, 0.1 mM PMSF, 25% glycerol [v/v]), incubated on ice for 20 min, and centrifuged for 5 min at 14,000 rpm at 4°C. The supernatant was used as the nuclear extract.

Electrophoresis mobility shift assay (EMSA)

The binding reaction mixture contained nuclear extract (5 μg of protein), 2 μg poly (dI-dC), and 10,000 cpm of a ^{32}P-labeled probe (oligonucleotide containing NF-κB binding site) in binding buffer (75 mM NaCl, 1.5 mM EDTA, 1.5 mM DTT, 7.5% glycerol, 1.5% NP-40, 15 mM Tris–HCl; pH 7.0). Samples were incubated for 20 min at RT in this mixture. DNA/protein complexes were separated

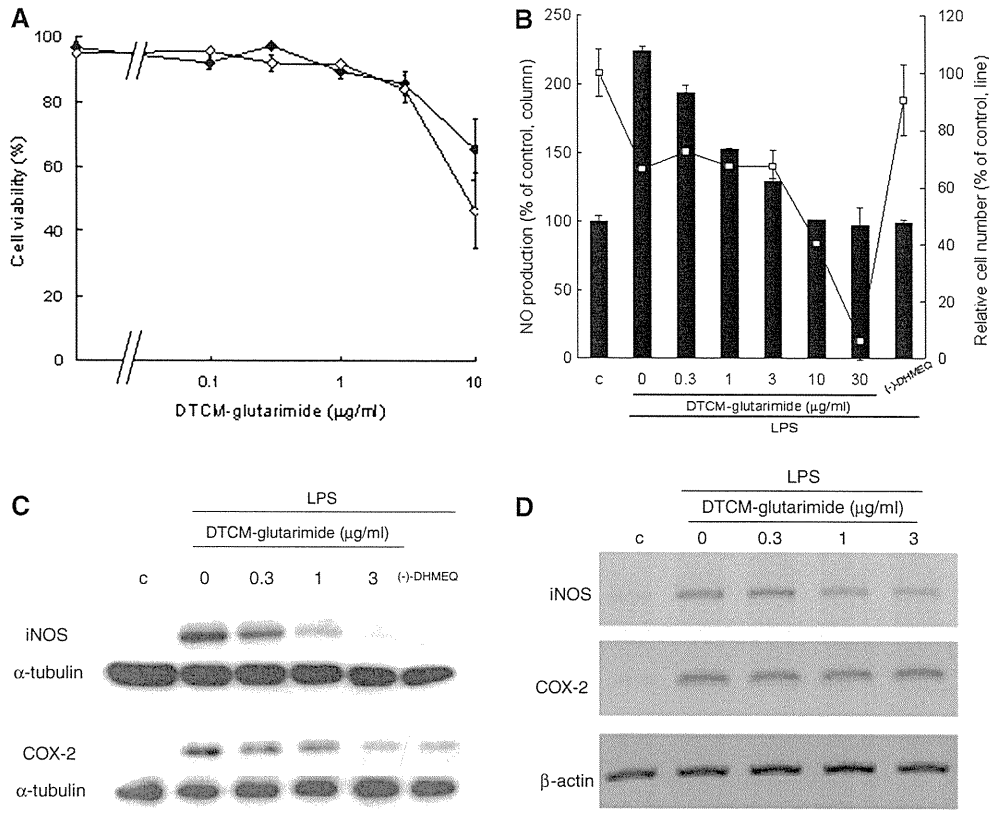

Fig. 2 Inhibition of LPS-induced NO production by DTCM-glutarimide. **a** Effect on cell viability. RAW264.7 cells were incubated with DTCM-glutarimide for 24 h (*black circles*) or 48 h (*white circles*). Cell viability was assessed by performing the trypan blue dye exclusion. The data are the mean ± SD of four determinations. The solvent control did not affect the cellular viability. **b** Inhibition of LPS-induced NO production. The cells were treated with DTCM-glutarimide or 10 μg/ml (−)-DHMEQ for 2 h, then stimulated with 3 μg/ml LPS and co-incubated with each drug for 20 h. NO production was measured by performing the Griess assay. The cell viability in the presence of LPS was measured by use of the MTT assay. The data are the mean ± SD of 3 determinations. **c** Inhibition by DTCM-glutarimide of LPS-induced expression of iNOS and COX-2. **d** Effect of DTCM-glutariomide on iNOS and COX-2 mRNA expression. The cells were treated with DTCM-glutarimide for 2 h, then stimulated with 3 μg/ml LPS and co-incubated with drug for 20 h

from free DNA on 4% native polyacrylamide gel in 0.25 mM TBE buffer. The DNA probes used for NF-κB binding were purchased from Promega (Madison, WI, USA). The following sequences were used as the NF-κB binding site: 5′-AGT TGA GGG GAC TTT CCC AGG C and 5′-GCC TGG GAA AGT CCC CTC AAC T. These oligonucleotides were labeled with [γ-^{32}P]-ATP (3,000 Ci/mmol; GE Healthcare, Little Chalfont, UK) by use of T4 polynucleotide kinase (Takara, Shiga, Japan), and purified by passage through a Nick column (GE Healthcare, Little Chalfont, UK).

In vitro kinase assay

Recombinant human JNK1α1 (20 ng; Millipore, Billerica, MA, USA) was incubated with 10 μCi [γ-32P]-ATP (3000 Ci/mmol; GE Healthcare, Little Chalfont, UK), 50 μM ATP (Sigma, St. Louis, MO, USA), and 2 μg recombinant human c-Jun (Sigma) in 30 μl of kinase buffer (20 mM HEPES, 10 mM MgCl2, 1 mM DTT, 1% Phosphatase Inhibitor Cocktail 2 [Sigma]). Reactions were incubated at 30°C for 1 h and terminated by the addition of Laemmli loading buffer. Proteins were separated by 10% SDS-PAGE, and phosphorylation was visualized by autoradiography.

Lymphocyte stimulation and mixed lymphocyte reaction assay

Purified C57BL/6 mouse-T cells (5×10^5/well) were stimulated with anti-CD28 (1 μg/ml) and plate pre-coated anti-CD3 (10 μg/ml) monoclonal antibodies, and were cultured in 96-well flat-bottomed plates (Costar, NY, USA). For mixed lymphocyte cultures (MLCs), irradiated (30 Gy, ^{137}Cs) BALB/c mouse splenocytes (5×10^5/well) were co-cultured with C57BL/6 mouse splenocytes (5×10^5/well) in 96-well round-bottomed plates (Corning). The plates were incubated at 37°C under 5% CO_2 plus

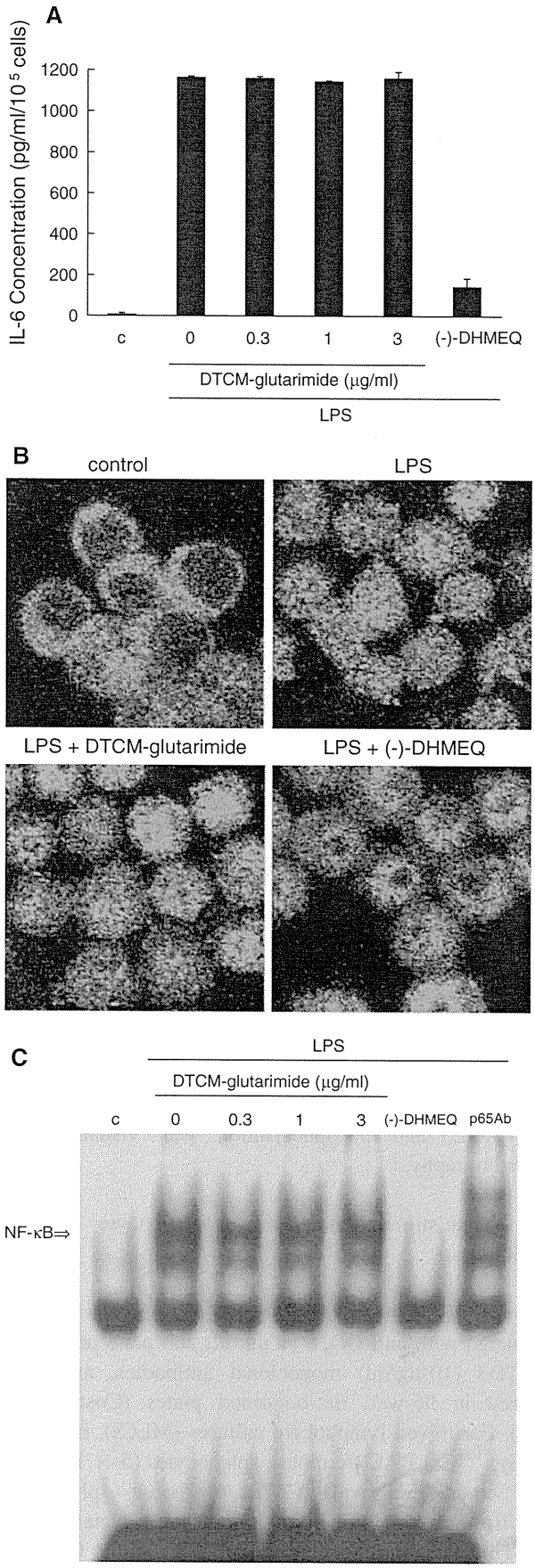

Fig. 3 Lack of NF-κB inhibition by DTCM-glutarimide. **a** Effect on LPS-induced IL-6 secretion. RAW264.7 cells were pretreated with DTCM-glutarimide or 10 μg/ml (−)-DHMEQ, and then stimulated with 3 μg/ml LPS and co-incubated with each drug for 20 h. IL-6 secretion was assessed by performing an ELISA. The data are the mean ± SD of three determinations. **b** Effect on LPS-induced NF-κB nuclear translocation. The cells were pretreated with 3 μg/ml DTCM-glutarimide or (−)-DHMEQ, and stimulated with LPS and co-incubated with each drug for 30 min. Then they were stained with p65 antibody, and analyzed by fluorescence microscopy. **c** Effect on LPS-induced NF-κB activation assessed by use of the EMSA. Nuclear extracts were prepared, and then mixed and incubated with a ^{32}P-labeled NF-κB probe for 20 min in the presence or absence of antibody against p65

air. Cells were pulsed with ^{3}H-thymidine (1 μCi/well) for 16 h before culture termination, and ^{3}H-thymidine incorporation was measured by using a β-counter (PerkinElmer, Boston, MA, USA).

Cardiac transplantation and treatment protocol

Male C57BL/6 (H-2^{b}) and BALB/c (H-2^{d}) mice (SLC Inc., Shizuoka, Japan) was used as donor and recipient, respectively. Heterotopic heart transplantation was performed according to the method previously described by Corry et al. [11]. Cardiac recipients were treated with either DTCM-glutarimide (10–60 mg/kg/day) or control vehicle (0.5% CMC). These agents were administered intraperitoneally, from day 0 to day 13. Graft beating was monitored by daily palpation, and was scored +1 to +4 based on the strength of graft contraction. Rejection was defined as cessation of beating, which was confirmed by direct inspection followed by histopathologic examination. Graft survival time was plotted by the Kaplan–Meier method, and a log-rank test was applied for comparison. A P value of less than 0.05 was considered statistically significant.

The animal experiments were approved by the Institutional Animal Care and Use Committee, and were conducted under the guidelines of our animal care policy.

Histology and immunohistochemistry

Cardiac graft was excised at the time of animal death. Tissues were fixed in 10% formalin, embedded in paraffin, and stained with hematoxylin and eosin (H&E). Graft samples were also embedded in an optimal cutting temperature compound, frozen in liquid nitrogen, and stored at −80°C. Frozen sections were stained with anti-CD4 (GK1.5: Santa Cruz Biotechnology, Santa Cruz, CA) and CD8 (KT15: AbD Serotec, Oxford, UK) Abs using the avidin–biotin complex method as previously described [12]. Positive cells were counted in three different high power fields (HPFs; magnification ×400).

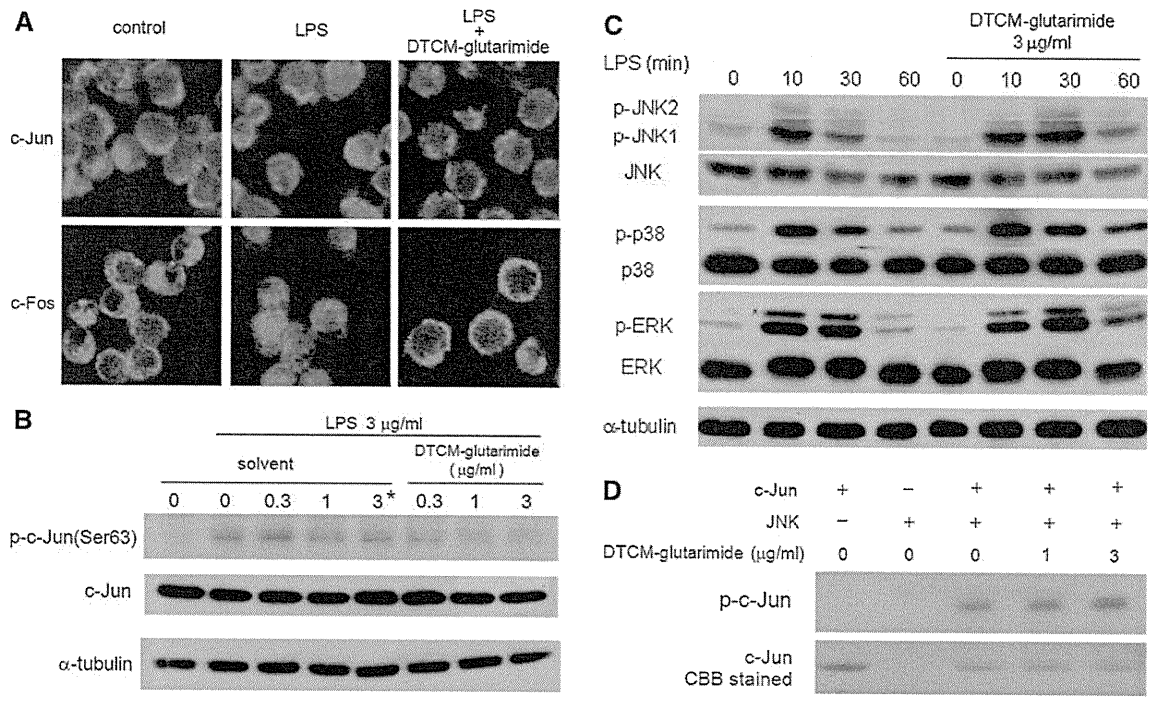

Fig. 4 Inhibition of LPS-induced AP-1 activation by DTCM-glutarimide. **a** Inhibition of LPS-induced nuclear translocation of c-Jun and c-Fos. Cells were pretreated or not with 3 μg/ml DTCM-glutarimide, stimulated or not with LPS and co-incubated with each drug for 30 min, and then analyzed by fluorescence microscopy. **b** Inhibition of c-Jun phosphorylation. Total cell extracts or nuclear extracts were prepared for Western blotting analysis. The proteins were immunoblotted with the indicated antibodies. The asterisk indicates the effect of DMSO alone at 0.3, 1, and 3 μg/ml DTCM-glutarimide; 0.3 (3 μl/ml), 1 (10 μl/ml), and 3 (30 μl/ml). **c** Effect on LPS-induced activation of MAPKs. Activation of MAPK proteins was measured in terms of the phosphorylation of each protein, as assessed by Western blot analysis. **d** Effect on JNK activity in vitro. Recombinant JNK1 and c-Jun were incubated with radioactive ATP for 1 h. Proteins were separated by SDS-PAGE, and phosphorylated c-Jun was visualized by autoradiography

Results

Inhibition of LPS-induced NO production and iNOS expression by DTCM-glutarimide

As shown in Fig. 2a, DTCM-glutarimide did not decrease the viability of RAW264.7 cells after 24 or 48 h when used at concentrations below 3 μg/ml. DTCM-glutarimide at 1–3 μg/ml clearly inhibited the LPS-induced NO production without any toxicity, just as did the NF-κB inhibitor (−)-DHMEQ [1–3], as shown in Fig. 2b. NO is produced mainly by inducible NO synthase (iNOS). LPS induced iNOS expression, which was strongly inhibited by DTCM-glutarimide (Fig. 2c). As the mechanism of inhibition, DTCM-glutarimide inhibited the iNOS mRNA expression (Fig. 2d). The analog also inhibited LPS-induced cyclooxygenase (COX)-2 protein expression weakly, but it did not inhibit the mRNA expression.

Lack of NF-κB inhibition by DTCM-glutarimide

IL-6 secretion is highly dependent on NF-κB, especially in RAW264.7 cells. Unexpectedly, DTCM-glutarimide did not inhibit LPS-induced IL-6 secretion at all, unlike (−)-DHMEQ (Fig. 3a). Then we studied the inhibition of NF-κB and found that its nuclear translocation was not inhibited by DTCM-glutarimide, as shown in Fig. 3b. Furthermore, the LPS-induced activation of NF-κB detected by EMSA was not inhibited by the analog (Fig. 3c).

Inhibition of LPS-induced AP-1 activation by DTCM-glutarimide

iNOS expression is positively regulated by transcription factors including NF-κB and also AP-1 [13]. LPS induced the nuclear translocation of AP-1 components c-Jun and c-Fos in RAW264.7 cells, and DTCM-glutarimide at 3 μg/ml clearly inhibited this translocation of both of them in the immunofluorescence assay, as shown in Fig. 4a. The phosphorylation of AP-1 components is known to occur before their nuclear translocation. By Western blot analysis, we found that DTCM-glutarimide inhibited the phosphorylation of c-Jun (Fig. 4b). In Fig. 4b, we confirmed the effect of solvent alone to exclude the solvent effects. In other experiments, we used DMSO at lower

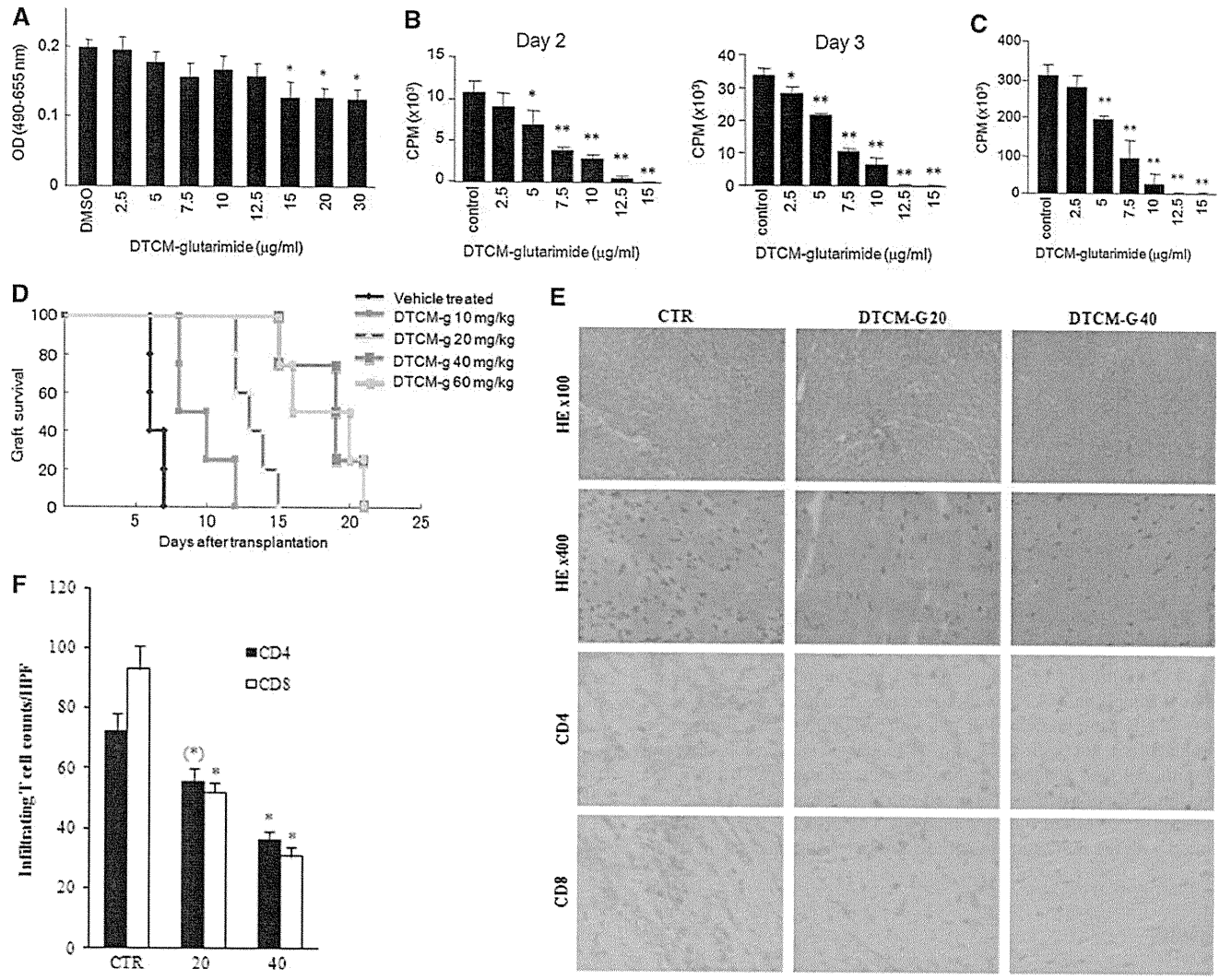

Fig. 5 Inhibition of mixed lymphocyte reaction and of graft rejection by DTCM-glutarimide. **a** Cytotoxicity of DTCM-glutarimide toward the responder C57BL/6 spleen cells. DTCM-glutarimide was added to the cells, which were then incubated for 6 h, after which the viability was assessed by performing the MTT assay. Values are the means and SD of three determinations. $*P < 0.05$. **b** Inhibition of the mixed lymphocyte reaction by mouse spleen cells. The responder C57BL/6 and stimulating BALB/c cells were co-cultured for 48 or 72 h. MLR was assessed by thymidine incorporation. Values are the means and SD of three or four determinations. $*P < 0.05$, $**P < 0.005$. **c** Inhibition of proliferation of purified T cells. Purified C57BL/6 T cells were stimulated with 1 μg/ml CD28 in plates precoated with anti-CD3 in the presence of DTCM-glutarimide for 48 h. The proliferation was measured by thymidine incorporation. Each value is the mean and SD of four4 determinations. $*P < 0.005$. **d** Inhibition of graft rejection by DTCM-glutarimide in mouse heart transplantation. As in the case of the donor/recipient strains of cells used in the MLR, the hearts of BALB/c (H-2d) mice were transplanted into C57BL/6 (H-2b) mice. DTCM-glutarimide at 10–60 mg/kg was given intraperitoneally every day from just before the transplantation. **e** Histology of cardiac grafts following transplantation. Cardiac allografts were stained with H&E (original magnification: ×100 or ×400), anti-CD4 (×400), or anti-CD8 Abs (×400). Representative photographs of four independent grafts on day 5 are shown. **f** The numbers of $CD4^+$ and $CD8^+$ cells in graft sections were counted in three different high power fields (HPF) and then quantified. Each bar represents the mean ± SEM of four independent experiments. $*P < 0.05$ versus control. (*CTR* control)

concentrations. On the other hand, it had no effect on the activation of MAPKs including p38, ERK, and JNK (Fig. 4c), so we expect that DTCM-glutarimide would inhibit the kinase activity of JNK. But it did not inhibit the phosphorylation of c-Jun by JNK in vitro (Fig. 4d). Thus, it is likely that DTCM-glutarimide would inhibit AP-1 activation by inhibition of the cofactors for JNK.

Inhibition of mixed lymphocyte reaction by DTCM-glutarimide

The mixed lymphocyte reaction (MLR) is known to be positively regulated by AP-1 [14, 15]. We employed spleen cells from C57BL/6 mice as responder cells and irradiated spleen cells from BALB/c mice as the stimulating cells.

Table 1 Amelioration of mouse cardiac allograft survival by DTCM-glutarimide treatment

DTCM-glutarimide (mg/kg)	N	Survival (days)	Median survival (days)
0	6	6, 6, 6, 6, 7, 7	6.0
10	4	8, 8, 10, 12	9.0#
20	4	12, 13, 14, 15	13.5#
40	4	15, 19, 19, 21	19.0#
60	4	15, 16, 20, 21	18.0#

# $P < 0.05$ versus control

When C57BL/6 spleen cells were incubated with DTCM-glutarimide for 6 h, their viability was not affected even at 12.5 μg/ml, as assessed by MTT analysis (Fig. 5a). The responder and stimulating cells were co-cultured for 48 or 72 h. DTCM-glutarimide at 5–12.5 μg/ml inhibited the MLR assessed by thymidine incorporation (Fig. 5b). As the MLR is dependent on responder T cell proliferation, we measured the effect of DTCM-glutarimide on the proliferation of C57BL/6 T cells purified by use of an enrichment column. The cells were then stimulated with anti-CD28 and anti-CD3 for 48 h. As shown in Fig. 5c, at concentrations of 5 μg/ml and above, DTCM-glutarimide inhibited the proliferation.

Inhibition of graft rejection by DTCM-glutarimide in mouse heart transplantation

The hearts of BALB/c (H-2d) mice were transplanted to C57BL/6 (H-2b) mice. DTCM-glutarimide at 10–60 mg/kg was given intraperitoneally every day from just before the transplantation. As shown in Fig. 5d and Table 1, at 10–40 mg/kg the analog prolonged the graft survival dose dependently. The effect appeared to be saturated at 40 mg/kg, and no toxicity was observed during the experiment even at 60 mg/kg. We also looked into the histology of cardiac sections. As shown in Fig. 5e and f, the numbers of CD4-positive and CD8-positive cells were reduced by the treatment of 20 or 40 mg/kg DTCM-glutarimide.

Discussion

The free radical NO produced by eNOS often plays an important role in regulating many physiological functions such as vasodilation and neurotransmission. However, overproduction of NO by iNOS in macrophages often provokes inflammatory diseases including atherosclerosis, rheumatoid arthritis, diabetes, septic shock, transplant rejection, and multiple sclerosis. Therefore, suppression of iNOS expression might be important for the treatment of inflammatory disorders [16, 17]. Since DTCM-glutarimide inhibits the expression of iNOS, it would be a possible candidate for use as an anti-inflammatory agent. Cyclooxygenase (COX) is a key enzyme catalyzing the rate-limiting step in the biosynthesis of prostaglandins from arachidonic acid [18, 19]. COX-2 often plays a key role in inflammation and also tumorigenesis [20, 21]. Because DTCM-glutarimide lowered the COX-2 expression (Fig. 2c), it may be a potential drug for treating inflammatory and neoplastic diseases.

Being a 9-methylstreptimidone derivative, DTCM-glutarimide inhibited the expression of iNOS and COX-2; but, unexpectedly, it did not inhibit the LPS-induced IL-6 secretion and NF-κB activation at all, unlike the NF-κB inhibitor (−)-DHMEQ (Fig. 3a–c). Next, we examined the effect of DTCM-glutarimide on the activation of AP-1, because the promoter regions of both the iNOS and COX-2 genes contain the binding sites for NF-κB and AP-1 [22, 23]. As shown in Fig. 4a–b, DTCM-glutarimide inhibited AP-1 activation at concentrations that inhibited NO production and the expression of iNOS and COX-2.

AP-1 is a heterodimer consisting of a member of the Jun family proteins and one of the Fos or ATF family proteins. A Jun/Jun homodimer is also possible [24]. The Jun family proteins include c-Jun, JunB, and JunD [24]; the Fos family ones, c-Fos, FosB, Fra-1, and Fra-2 [25–28]; and the ATF family ones, ATF-2, ATF-3/LRF1, and B-ATF [29–31]. Each AP-1 protein is phosphorylated in the cytoplasm, and enters the nucleus to form the dimer. The Jun/Fos complex mainly binds to the TPA-responsive element (TRE); and the Jun/ATF complex, to the cyclic AMP-responsive element (CRE; 24, 28). The c-Jun/c-Fos heterodimer is the most common form of AP-1.

Activation of JNK leads to the phosphorylation of c-Jun and an increase in the transcriptional activity of AP-1 [32]. Our finding that DTCM-glutarimide inhibited the cellular phosphorylation of c-Jun (Fig. 4b) indicates that the inhibition of AP-1 activation by this compound would be due to inhibition upstream of the c-Jun phosphorylation. We demonstrated that DTCM-glutarimide did not affect the activation of various MAPKs (Fig. 4c), and also did not inhibit the phosphorylation of recombinant c-Jun by recombinant JNK (Fig. 4d). Therefore, it is possible that DTCM-glutarimide would inhibit the cofactor activity of JNK. The effect of DTCM-glutarimide on AP-1 components other than c-Jun and the molecular target remain to be studied.

DTCM-glutarimide inhibited the MLR reaction and purified T-cell proliferation. Also, in the in vivo study, it increased the graft survival time of transplanted hearts in mice. The effective dose of DTCM-glutarimide at 10–60 mg/kg did not show any toxicity. Thus, DTCM-glutarimide may be stable in the animal body and

distributed widely to the organs. Histological observation indicated that treatment with DTCM-glutarimide lowers the number of CD4- and CD8-positive cells in the cardiac section. The mechanism of MLR inhibition and graft survival may also include some activity of DTCM-glutarimide other than AP-1 inhibition.

A small molecular weight AP-1 inhibitor, T-5224, was designed to interact with AP-1 proteins, and it inhibits rheumatoid arthritis in animals [33]. Compared with T-5224, DTCM-glutarimide is likely to inhibit AP-1 functions by a different mechanism. Moreover, having a simpler structure, it may be more advantageous than T-5224, because DTCM-glutarimide is more easily prepared.

In conclusion, DTCM-glutarimide inhibited the expression of iNOS and COX-2 in a mouse macrophage cell line RAW264.7. The effect may have been partly due to the inhibition of AP-1 activity. Furthermore, it extended the survival time of transplanted hearts in mice. Although the precise mechanism of its anti-inflammatory activity requires further studies, DTCM-glutarimide may be a new candidate as an anti-inflammatory agent.

Acknowledgments This work was financially supported in part by grants from the program Grants-in-Aid for Scientific Research on Priority Areas of the Ministry of Education, Culture, Sports, Science, and Technology (MEXT). It was also supported by a High-Tech Research Center Project for Private Universities: matching fund subsidy from MEXT, 2006–2011, and the Global Center of Excellence Program from MEXT, 2007–2012.

References

1. Matsumoto N, Ariga A, To-e S, Nakamura H, Agata N, Hirano S, et al. Synthesis of NF-kappaB activation inhibitors derived from epoxyquino- micin C. Bioorg Med Chem Lett. 2000;10:865–9.
2. Ariga A, Namekawa J, Matsumoto N, Inoue J, Umezawa K. Inhibition of tumor necrosis f actor-alpha-induced nuclear translocation and activation of NF-kappa B by dehydroxymethylepoxyquinomicin. J Biol Chem. 2002;277:24625–30.
3. Yamamoto M, Horie R, Takeiri M, Kozawa I, Umezawa K. Inactivation of NF-kappaB components by covalent binding of (−)-dehydroxymethylepoxyquinomicin to specific cysteine residues. J Med Chem. 2008;51:5780–8.
4. Watanabe M, Ohsugi T, Shoda M, Ishida T, Aizawa S, Maruyama-Nagai M, Utsunomiya A, Koga S, Yamada Y, Kamihira S, Okayama A, Kikuchi H, Uozumi K, Yamaguchi K, Higashihara M, Umezawa K, Watanabe T, Horie R. Dual targeting of transformed and untransformed HTLV-1-infected T-cells by DHMEQ, a potent and selective inhibitor of NF-κB, as a strategy for chemoprevention and therapy of adult T cell leukemia. Blood. 2005;106:2462–71.
5. Umezawa K. Inhibition of tumor growth by NF-κB inhibitors. Cancer Sci. 2006;97:990–5.
6. Hamasaka A, Yoshioka N, Abe R, Kishino S, Umezawa K, Ozaki M, Todo S, Shimizu H. Topical application of DHMEQ improves allergic inflammation via NF-κB inhibition. J Allergy Clin Immunol. 2010;126:400–3.
7. Ueki S, Yamashita K, Aoyagi T, Haga S, Suzuki T, Itoh T, et al. Control of allograft rejection by applying a novel nuclear factor-kappaB inhibitor, dehydroxymethylepoxy-quinomicin. Transplantation. 2006;82:1720–7.
8. Umezawa K. Screening of bioactive metabolites that suppress inflammation. Tanpakushitsu Kakusan Koso. 2007;52:1685–9.
9. Ishikawa Y, Tachibana M, Matsui C, Obata R, Umezawa K, Nishiyama S. Synthesis and biological evaluation on novel analogs of 9-methylstreptimidone, an inhibitor of NF-kappaB. Bioorg Med Chem Lett. 2009;19:1726–8.
10. Dignam JD, Lebovitz RM, Roeder RG. Accurate transcription initiation by RNA polymerase II in a soluble extract from isolated mammalian nuclei. Nucleic Acids Res. 1983;11:1475–89.
11. Corry RJ, Winn HJ, Russel PS. Primarily vascularized allografts of hearts in mice. The role of H-2D, H-2K, and non-H-2 antigens in rejection. Transplantation. 1973;16:343–50.
12. Nomura M, Yamashita K, Murakami M, Takehara M, Echizenya H, Sunahara M, et al. Induction of donor-specific tolerance by adenovirus-mediated CD40Ig gene therapy in rat liver transplantation. Transplantation. 2002;73(9):1403–10.
13. Jang JH, Surh YJ. AP-1 mediates beta-amyloid-induced iNOS expression in PC12 cells via the ERK2 and p38 MAPK signaling pathways. Biochem Biophys Res Commun. 2005;331:1421–8.
14. Yea SS, Jeong HS, Choi CY, Park KR, Oh S, Shin JG, et al. Inhibitory effect of anethole on T-lymphocyte proliferation and interleukin-2 production through down-regulation of the NF-AT and AP-1. Toxicol In Vitro. 2006;20:1098–105.
15. Thornton TM, Zullo AJ, Williams KL, Taparowsky EJ. Direct manipulation of activator protein-1 controls thymocyte proliferation in vitro. Eur J Immunol. 2006;36:160–9.
16. Park PH, Kim HS, Jin XY, Jin F, Hur J, Ko G, et al. KB-34, a newly synthesized chalcone derivative, inhibits lipopolysaccharide-stimulated nitric oxide production in RAW 264.7 macrophages via heme oxygenase-1 induction and blockade of activator protein-1. Eur J Pharmacol. 2009;606:215–24.
17. Chen CY, Peng WH, Tsai KD, Hsu SL. Luteolin suppresses inflammation-associated gene expression by blocking NF-kappaB and AP-1 activation pathway in mouse alveolar macrophages. Life Sci. 2007;81:1602–14.
18. Smith WL, Garavito RM, DeWitt DL. Prostaglandin endoperoxide H synthases (cyclooxygenases)-1 and -2. J Biol Chem. 1996;271:33157–60.
19. Herschman HR. Prostaglandin synthase 2. Biochim Biophys Acta. 1996;1299:125–40.
20. Vane JR, Bakhle YS, Botting RM. Cyclooxygenases 1 and 2. Annu Rev Pharmacol Toxicol. 1998;38:97–120.
21. Dubois RN, Abramson SB, Crofford L, Gupta RA, Simon LS, Van De Putte LB, et al. Cyclooxygenase in biology and disease. FASEB J. 1998;12:1063–73.
22. Lowenstein CJ, Alley EW, Raval P, Snowman AM, Snyder SH, Russell SW, et al. Macrophage nitric oxide synthase gene: two upstream regions mediate induction by interferon gamma and lipopolysaccharide. Proc Natl Acad Sci USA. 1993;90:9730–4.
23. Yao J, Mackman N, Edgington TS, Fan ST. Inhibitory effect of 1,8-cineol (eucalyptol) on Egr-1 expression in lipopolysaccharide-stimulated THP-1 cells. J Biol Chem. 1997;272:17795–801.
24. Nakabeppu Y, Ryder K, Nathans D. DNA binding activities of three murine Jun proteins: stimulation by Fos. Cell. 1988;5:907–15.
25. Ryseck RP, Kovary K, Bravo R. Integrity of FOS B leucine zipper is essential for its interaction with JUN proteins. Oncogene. 1990;5:1091–3.
26. Cohen DR, Curran T. fra-1: a serum-inducible, cellular immediate-early gene that encodes a fos-related antigen. Mol Cell Biol. 1988;8:2063–9.

27. Nishina H, Sato H, Suzuki T, Sato M, Iba H. Isolation and characterization of fra-2, an additional member of the fos gene family. Proc Natl Acad Sci USA. 1990;87:3619–23.
28. Chiu R, Boyle WJ, Meek J, Smeal T, Hunter T, Karin M. The c-Fos protein interacts with c-Jun/AP-1 to stimulate transcription of AP-1 responsive genes. Cell. 1988;54:541–52.
29. Macgregor PF, Abate C, Curran T. Direct cloning of leucine zipper proteins: Jun binds cooperatively to the CRE with CRE-BP1. Oncogene. 1990;5:451–8.
30. Hsu JC, Laz T, Mohn KL, Taub R. Identification of LRF-1, a leucine-zipper protein that is rapidly and highly induced in regenerating liver. Proc Natl Acad Sci USA. 1991;88:3511–5.
31. Dorsey MJ, Tae HJ, Sollenberger KG, Mascarenhas NT, Johansen LM, Taparowsky EJ. B-ATF: a novel human bZIP protein that associates with members of the AP-1 transcription factor family. Oncogene. 1995;11:2255–65.
32. Dérijard B, Hibi M, Wu IH, Barrett T, Su B, Deng T, Karin M, Davis RJ. JNK1: a protein kinase stimulated by UV light and Ha-Ras that binds and phosphorylates the c-Jun activation domain. Cell. 1994;76:1025–37.
33. Aikawa Y, Morimoto K, Yamamoto T, Chaki H, Hashiramoto A, Narita H, Hirono S, Shiozawa S. Treatment of arthritis with a selective inhibitor of c-Fos/activator protein-1. Nat Biotechnol. 2008;26:817–23.

Cancer Science
The official journal of the Japanese Cancer Association JCA

Inhibition of nuclear factor-kappaB suppresses peritoneal dissemination of gastric cancer by blocking cancer cell adhesion

Kazuhiro Mino,[1] Michitaka Ozaki,[2,7] Kazuaki Nakanishi,[1] Sanae Haga,[2,3] Masanori Sato,[1] Masaya Kina,[1] Masato Takahashi,[1] Norihiko Takahashi,[1] Akihiko Kataoka,[1] Kazuyoshi Yanagihara,[4] Takahiro Ochiya,[5] Toshiya Kamiyama,[1] Kazuo Umezawa[6] and Satoru Todo[1]

[1]Department of General Surgery, Graduate School of Medicine, Hokkaido University, Sapporo; [2]Department of Molecular Surgery, Hokkaido University School of Medicine, Sapporo; [3]The Japan Society for the Promotion of Science (JSPS), Tokyo; [4]Department of Life Sciences, Yasuda Women's University Faculty of Pharmacy, Hiroshima; [5]Section for Studies on Metastasis, National Cancer Center Research Institute, Tokyo; [6]Department of Applied Chemistry, Faculty of Science and Technology, Keio University, Yokohama, Japan

(Received November 4, 2010/Revised January 24, 2011/Accepted January 25, 2011/Accepted manuscript online February 2, 2011/Article first published online March 1, 2011)

Currently, patients with peritoneal dissemination of gastric cancer must accept a poor prognosis because there is no standard effective therapy. To inhibit peritoneal dissemination it is important to inhibit interactions between extracellular matrices (ECM) and cell surface integrins, which are important for cancer cell adhesion. Although nuclear factor-kappa B (NF-κB) is involved in various processes in cancer progression, its involvement in the expression of integrins has not been elucidated. We used a novel NF-κB inhibitor, dehydroxymethylepoxyquinomicin (DHMEQ), to study whether NF-κB blocks cancer cell adhesion via integrins in a gastric cancer dissemination model in mice and found that DHMEQ is a potent suppressor of cancer cell dissemination. Dehydroxymethylepoxyquinomicin suppressed the NF-κB activity of human gastric cancer cells NUGC-4 and 44As3Luc and blocked the adhesion of cancer cells to ECM when compared with the control. Dehydroxymethylepoxyquinomicin also inhibited expression of integrin (α2, α3, β1) in *in vitro* studies. In the *in vivo* model, we injected 44As3Luc cells pretreated with DHMEQ into the peritoneal cavity of mice and performed peritoneal lavage after the injection of cancer cells. Viable cancer cells in the peritoneal cavities were evaluated sequentially by *in vivo* imaging. In mice injected with DHMEQ-pretreated cells and lavaged, live cancer cells in the peritoneum were significantly reduced compared with the control, and these mice survived longer. These results indicate that DHMEQ could inhibit cancer cell adhesion to the peritoneum possibly by suppressing integrin expression. Nuclear factor-kappa B inhibition may be a new therapeutic option for suppressing postoperative cancer dissemination. (*Cancer Sci* 2011; 102: 1052–1058)

Peritoneal dissemination is the most frequent process through which gastric cancer recurs,[1] and patients with this condition must currently accept a very poor prognosis.[2,3] Standard chemotherapy is currently not sufficiently effective for improving the survival of patients with peritoneal dissemination of gastric cancer. To inhibit peritoneal dissemination, it may be important to control the adhesion of cancer cells to the peritoneum. During cancer cell dissemination in the abdominal cavity, cancer cells make contact with the basement membrane through gaps between mesothelial cells.[4,5] The basement membrane beneath mesothelial cells comprises extracellular matrices (ECM) consisting of type 1 and 4 collagen, fibronectin or laminin,[6] and mesothelial cells also produce ECM.[7] The interactions between these ECM and cell surface integrins play very important roles in cancer cell adhesion and, therefore, cancer progression.[8]

Integrins are membrane-bound proteins that form heterodimers of α- and β-subunits at the cell surface. The α-subunits vary between 120 and 180 kD, and are non-covalently associated with β-subunits (90–110 kD). To date, 14 α subunits and eight β subunits have been identified, and after mutual dimerization, these subunits contribute to cell adhesion or regulation of signal transduction required for cell survival by making contact with appropriate ECM.[9,10] It has been reported that integrins α2, α3 and β1 play important roles in the peritoneal dissemination of gastric cancer,[11] and that antibodies to these integrins suppress peritoneal dissemination of gastric cancer in a mouse model.[12]

Nuclear factor-kappaB (NF-κB) was first identified and reported in 1986[13] and studied in the context of immune and inflammatory responses.[14] Nuclear factor-kappaB is a generic term for dimers of NF-κB1 (p50/p105), NF-κB2 (p52/p100), c-Rel, RelA (p65/NF-κB3) and RelB.[15] To date, involvement of NF-κB in cancer-related molecules such as cyclin D1,[16] intercellular adhesion molecule-1 (ICAM-1), vascular cell adhesion molecule-1 (VCAM-1),[17] the Bcl family,[18] inhibitor of apoptosis (IAP), X-linked inhibitor of apoptosis protein (XIAP),[19] p53,[20] vascular endothelial growth factor (VEGF), interleukin (IL)-8,[21] MMP[22] and multidrug resistance protein 1 (MDR1),[23] has been elucidated. However, NF-κB has not been reported to be involved in cancer cell adhesion to the peritoneum via integrins.

A low-molecular-weight NF-κB inhibitor, dehydroxymethylepoxyquinomicin (DHMEQ), was newly developed by Umezawa.[24] Dehydroxymethylepoxyquinomicin specifically inhibits the nuclear translocation of p65 and prevents it binding to DNA[25]; it also has various anti-cancer effects in mouse models without obvious side-effects. Thus far, the following anti-cancer effects of DHMEQ have been reported: G1 arrest by inhibition of cyclin D1 expression;[26] and induction of apoptosis by inhibition of cIAP and XIAP,[27] or Bcl-2 and Bcl-xL.[28] Antitumor effects of DHMEQ have also been reported in *in vivo* models such as those for thyroid cancer,[27] prostate cancer,[29] hepatic cancer,[30] breast cancer,[31] pancreas cancer,[32] multiple myeloma,[28] malignant lymphoma[33] and leukemia.[26]

In the present study, we showed that NF-κB is associated with integrin expression in gastric cancer cell lines and that NF-κB inhibition by DHMEQ suppresses cancer progression by inhibiting the adhesion of gastric cancer cells to the peritoneum in a mouse model of peritoneal dissemination of gastric cancer.

[7]To whom correspondence should be addressed.
E-mail: ozaki-m@med.hokudai.ac.jp

doi: 10.1111/j.1349-7006.2011.01901.x

Materials and Methods

Cell cultures. The human gastric cancer cell line NUGC4 was obtained from the Japanese Cancer Research Resources Bank (JCRB, Osaka, Japan), and 44As3Luc with luciferase activity was constructed by one of the authors (K.Y.).[34] The 44As3Luc cells were derived from 44As3 cells, which is a highly peritoneal metastatic cell line, and were stably transfected with a pEGF-PLuc plasmid with CMV promoter (Clontech, Palo Alto, CA, USA). Human breast cancer cell lines MCF7 with constitutively low NF-κB activity and MDA-MB231 with constitutively high NF-κB activity were obtained from the American Type Culture Collection (Rockville, MD, USA).[31] The NUGC4 cells were cultured at 37°C in RPMI1640 (Sigma, St Louis, MO, USA) along with 10% fetal bovine serum (FBS); the 44As3Luc cells were cultured at the same temperature with RPMI1640 containing 100 μg/mL geneticin (Sigma); and the MCF7 and MDA-MB231 cells were also cultured at 37°C in 95% air and 5% CO_2 in DMEM (Sigma) along with 10% FBS.

Dehydroxymethylepoxyquinomycin (DHMEQ). We have originally designed and developed DHMEQ (molecular weight (MW): 261), a derivative of the natural antibiotic epoxyquinomycin C, to specifically target NF-κB.[24]

DNA-binding activity of NF-κB. To evaluate the DNA-binding activity of NF-κB in the steady state, 70% confluent cultures of NUGC4, 44As3Luc, MCF7 and MDA-MB231 in 10-cm dishes were stored at −80°C. To evaluate the effect of DHMEQ, the medium in the 70% confluent cultures of NUGC4 and 44As3Luc was replaced with 10 μg/mL DHMEQ solution, incubated for an appropriate time and stored at −80°C. The following day, nuclear proteins were extracted and examined using a p65 TransAM kit (ActiveMotif, Carlsbad, CA, USA). The absorbance was determined using a plate reader (Varioskan Flash, Thermo Fisher Scientific, Waltham, MA, USA). Each experiment was performed in triplicate.

NF-κB reporter gene assay. A GFP reporter gene construct was transfected using Cignal Reporter Assay kits (SA Biosciences, Frederick, MD, USA). Cultured cells were trypsinized and resuspended in Opti-MEM (Invitrogen, Carlsbad, CA, USA) with non-essential amino acids (Invitrogen) without antibiotics at a concentration of 2×10^5 cells in a 96-well plate. Cells were transfected with the reporter by culturing for 16 h with Surefect (SA Biosciences). After the medium was replaced with Opti-MEM with penicillin/streptomycin, the cells were incubated for an additional 8 h. The medium was then replaced with Opti-MEM containing 10 μg/mL of DHMEQ (or 0.024% of DMSO for the controls). The intensity of fluorescence was measured at appropriate times in triplicate using Varioskan Flash (excitation, 470 nm; emission, 515 nm).

mRNA expression of integrins in DHMEQ-treated cells. Real-time PCR was used to examine mRNA expression. The 44As3Luc cells were cultured in triplicate in 0.024% DMSO solution (controls) or in 10 μg/mL DHMEQ for the appropriate times. Total RNA was isolated using an RNeasy mini kit (Qiagen, Valencia, CA, USA) in accordance with the manufacturer's instructions. For cDNA synthesis, ReverTra Ace qPCR RT kit (Toyobo, Osaka, Japan) with Oligo(dT) 20 primer (Toyobo) was used in accordance with the manufacturer's instructions. For relative quantification by PCR, each cDNA product was analyzed in a LightCycler (version 1.4) using a QuantiTect SYBR Green PCR kit (Qiagen).

Flow cytometric analysis of integrin expression. p65 silencing was performed using p65 siRNA2 (BD Biosciences, Bedford, MA, USA). Next, 50% confluent cells were incubated for 24 h in medium without antibiotics in 10-cm dishes. Then, 33 nM p65 siRNA was added to each dish and transfected for 48 h. p65 silencing was confirmed by western blot analysis using primary antibodies against ×500 α-tubulin and ×1000 p65 protein (Cell Signaling, Beverly, MA, USA) and ×5000 goat anti-mouse IgG for tubulin or anti-rabbit IgG for the p65 protein. With regard to DHMEQ treatment, the medium in 70% confluent cell cultures in 10-cm dishes was replaced with 10 μg/mL DHMEQ solution (0.024% DMSO for the controls) and cultured for the appropriate times. These cells were trypsinized and analyzed using flow cytometry (FACS Caliber; Becton Dickinson, Franklin Lakes, NJ, USA). The antibodies used for these assays were integrin α2, integrin α3, integrin β1 and isotype controls for these integrins. All antibodies were obtained from R&D Systems (Minneapolis, MN, USA).

Adhesion assay. We evaluated the anti-adhesive effect of DHMEQ by using a plate pre-coated with ECM constituting the peritoneal basement membrane. The medium in 70% confluent cell cultures in 10-cm dishes was replaced with 10 μg/mL DHMEQ solution (or 0.024% DMSO for the controls), and the dishes were incubated for 24 h. These cells were trypsinized, assembled, adjusted to a concentration of 1×10^6 cells/mL with RPMI and distributed on the pre-coated plates (80 μL per plate). Next, the cells were incubated at 37°C for 1 h. Except for the non-treated plate, all plates were washed three times with 100 μL of FBS-free RPMI. After washing, 10 μL of ×50 diluted Cell Counting kit F (CCKF; Dojindo, Osaka, Japan) was added to each well, and the fluorescence intensity of the remaining live cells (adhesive cells) was evaluated using Varioskan Flash at 30 min after CCKF administration (excitation, 490 nm; emission, 515 nm). Pre-coated plates were manufactured by BD Biosciences and the ECM coated on the plates were types 1 and 4 collagen, fibronectin and laminin.

DHMEQ cytotoxicity assay. The cells were seeded into 96-well plates at 5×10^3 cells/well in 10% FBS-containing medium. Twenty-four hours later, the medium in the wells was replaced with different concentrations of DHMEQ solution or 0.048% DMSO solution, and the cells were then incubated again for 24 h. Lactate dehydrogenase (LDH) activity of the supernatant was measured using an LDH cytotoxicity detection kit (Takara Bio, Shiga, Japan).

Animal experiments. Six-week-old male BALB/c-nu/nu mice, each weighing approximately 20 g, were obtained from CLEA Japan, Inc. (Tokyo, Japan). The mice were grouped as follows: (i), implantation of DMSO-treated cells; (ii) implantation of DHMEQ-treated cells; (iii) implantation of DMSO-treated cells with peritoneal lavage; and (iv) implantation of DHMEQ-treated cells with peritoneal lavage. Each group comprised four mice. Then, 2×10^6 44As3Luc cells, which had been treated with 10 μg/mL DHMEQ (or 0.024% DMSO for the controls) for 24 h, were injected intraperitoneally into the above mentioned mice. One hour after injection, laparotomy and peritoneal lavage were performed using phosphate-buffered saline (PBS). Peritoneal lavage was performed through a 1-cm incision through which 5 mL of PBS was slowly injected. Bio-imaging was performed before and after the peritoneal lavage, and on days 2, 5, 10, 15 and 20 in order to evaluate cancer progression. Luminescence was evaluated at approximately 7 min after intraperitoneal injection of 1500 μg/mouse D-luciferin potassium salt (Synchem OHG, Altenburg, Germany). *In vivo* imaging was performed using Photon Imager Hu (Biospace Lab, Paris, France) with the mice under isoflurane anesthesia (Abbott Japan, Tokyo, Japan). Images were captured using Photo Acquisition 2.6 (Biospace Lab) with 0.5 min exposure and processed using Photo Vision Plus. Signal intensity was quantified as the sum of all detected photon counts (count per minute [CPM]) within the region of interest (ROI). All procedures involving animals and their care were approved by the Ethics Committee of Hokkaido University in accordance with institutional and Japanese governmental guidelines for animal experiments.

Scanning electron microscopy (SEM) of the peritoneal wall. The peritoneal walls of mice injected with cancer cells

were fixed with 10% formaldehyde for 180 min and then overnight at 4°C with 1.25% glutaraldehyde solution. The fixed samples were dehydrated in a 30–100% graded ethanol series and immersed in tert-butyl alcohol overnight at −20°C. These samples were dried using ES-2000 (Hitachi High-Technologies Co., Tokyo, Japan) for 3 h and ion-sputtered using E-1030 (Hitachi) for 120 s. The peritoneal surface was observed under a scanning electron microscope (S-3500N; Hitachi).

Statistics. The mean and SD were calculated for all variables, except the data from the flow cytometry. Between-group statistical significance was determined using the Student's *t* test. $P < 0.05$ was considered as statistically significant.

Results

DHMEQ effectively suppresses p65-DNA binding activity in gastric cancer cells. In the steady state, the p65-DNA binding activities in NUGC4 and 44As3Luc cells were as high as that in MDA-MB231 cells, a positive control cell with high binding activity. The activity in MCF7 cells is constitutively low as previously reported [31], and hence these cells were used as the negative control (Fig. 1A). The binding activities in both cells reached their lowest levels 2 h after the addition of 10 μg/mL DHMEQ (as a final concentration) and returned to initial conditions within 24 h (Fig. 1B). A GFP reporter assay showed that DHMEQ significantly suppresses transcriptional activity in both cells (Fig. 1C). On the basis of these results, we considered that DHMEQ had a similar effect in NUGC4 and 44As3Luc cells. Therefore, we used 44As3Luc cells in the following experiments. We planned to evaluate cancer progression using bioimaging.

Effect of NF-κB inhibition on integrin expression. In 44As3Luc cells, the mRNA of all integrins – α2, α3 and β1 – were significantly suppressed 2 h after the addition of 10 μg/mL DHMEQ (as a final concentration) compared with the control to which DMSO was added (Fig. 2A). The percentage reduction in the expressions of integrins α2, α3 and β1 was 27%, 31% and 8%, respectively. Flow cytometric analysis revealed that the expressions of all cell surface integrins on 44As3Luc cells were gradually suppressed after the addition of DHMEQ (Fig. 2B). Reductions in integrin expression (α2, α3 and β1) following DHMEQ addition was 68%, 83% and 45% at 24 h, respectively. Similarly, flow cytometric analysis of integrins α2, α3 and β1 revealed that the expressions of cell surface integrins in p65-deleted cells were suppressed to the same degree as in DHMEQ-treated cells (Fig. 2C). Reductions in integrin expression after p65 deletion were 34% (α2), 76% (α3) and 41% (β1). p65 silencing was confirmed by western blotting for nuclear and cytoplasmic p65 proteins (Fig. 2D).

Anti-adhesive effect of DHMEQ-treated cells in an *in vitro* assay. Significantly fewer 44As3Luc cells treated with 10 μg/mL DHMEQ (final concentration) remained alive on plates pre-coated with ECM after they were washed (ECM-adhesive cells) than 44As3Luc cells treated with DMSO (Fig. 3A). Reductions in the numbers of adhesive cells following DHMEQ addition were 18.3% (laminin), 34.8% (fibronectin), 38.2% (type 1 collagen) and 43.5% (type 4 collagen). The LDH value, which represents the cytotoxic effect, was significantly elevated in the supernatant of cells treated with DHMEQ at concentrations >17.5 μg/mL (Fig. 3B).

Effect of peritoneal lavage on implantation of DHMEQ-treated cancer cells on the abdominal wall. The number of cancer cells decreased in mice injected with DHMEQ-pretreated cells and subjected to peritoneal lavage (Fig. 4A). The intensity of bioluminescence after lavage was significantly reduced (reduction rate, 39%) in mice that were injected with DHMEQ-pretreated cells and subjected to peritoneal lavage compared with in mice injected with DMSO-pretreated control cells and subjected to

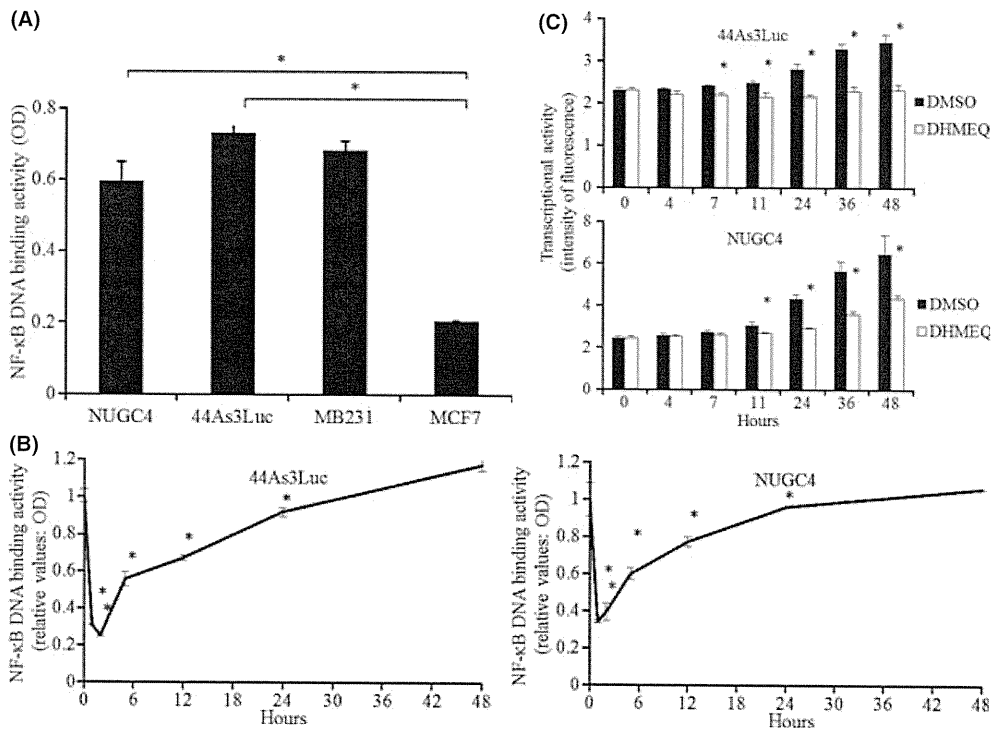

Fig. 1. Dehydroxymethylepoxyquinomicin (DHMEQ) effectively suppressed p65-DNA binding activity in gastric cancer cells. (A) Nuclear p65 protein binding activity to DNA in a steady state. MDA-MB231 cells were used as a positive control, and MCF7 cells were used as a negative one. *$P < 0.05$. (B) Time course of binding activity of nuclear p65 proteins to DNA in DHMEQ-treated cells. The binding activities of both cells were assessed at 2, 6, 12, 24 and 48 h after DHMEQ administration. *Significantly <0 h ($P < 0.05$). (C) Nuclear factor-kappa B (NF-κB) GFP reporter assay. The black bars show cells treated with DMSO, and white bars show those with DHMEQ. *Significantly more than controls ($P < 0.05$). OD, optical density.

doi: 10.1111/j.1349-7006.2011.01901.x

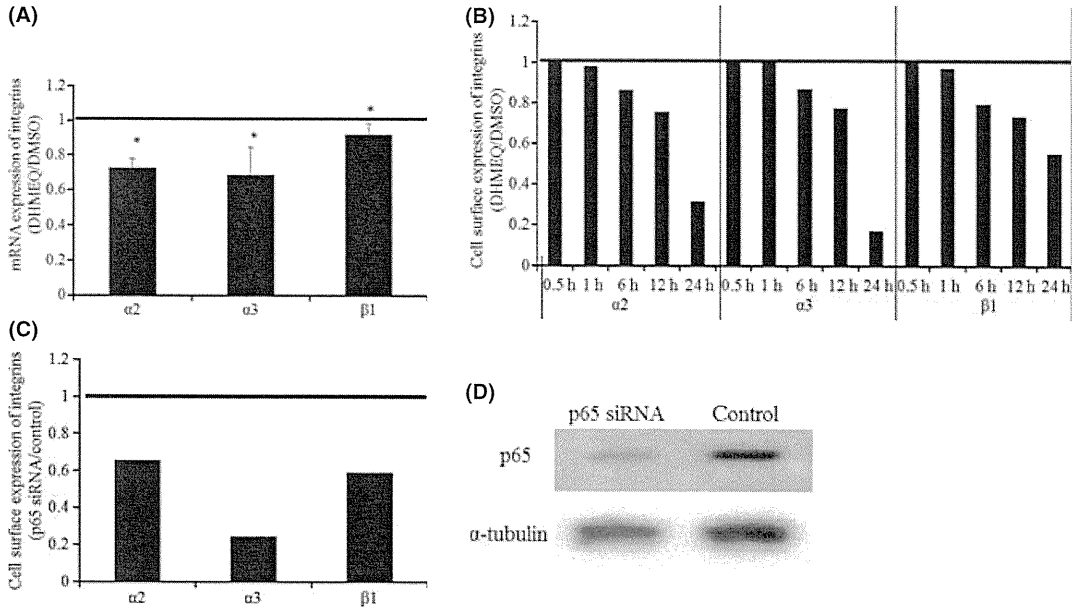

Fig. 2. Effect of nuclear factor-kappa B (NF-κB) inhibition on expression of adhesion molecules. (A) Quantitative evaluation of mRNA of integrins by real-time PCR. The graph shows the average of the ratio of copies of dehydroxymethylepoxyquinomicin (DHMEQ)-treated 44As3Luc cells to DMSO-treated cells at 2 h after DHMEQ administration. When the longitudinal value is below 1 (bold line), the integrin expression of DHMEQ-treated cells is lower than that of DMSO-treated cells. *Significantly less than controls ($P < 0.05$). (B) Expression of cell surface integrins of DHMEQ-treated cells. The graph shows the expression rate of cell surface adhesion molecules of 44As3Luc cells treated with DHMEQ compared with that of DMSO-treated cells for each time point. The bold line is as described above. (C) Expression of cell surface adhesion molecules of cells knocked down by p65 siRNA. The graph shows the rate of cell surface integrins of 44As3Luc cells knocked down by p65 siRNA. The bold line is as described above. (D) p65 deletion. The p65 deletion was confirmed by western blotting.

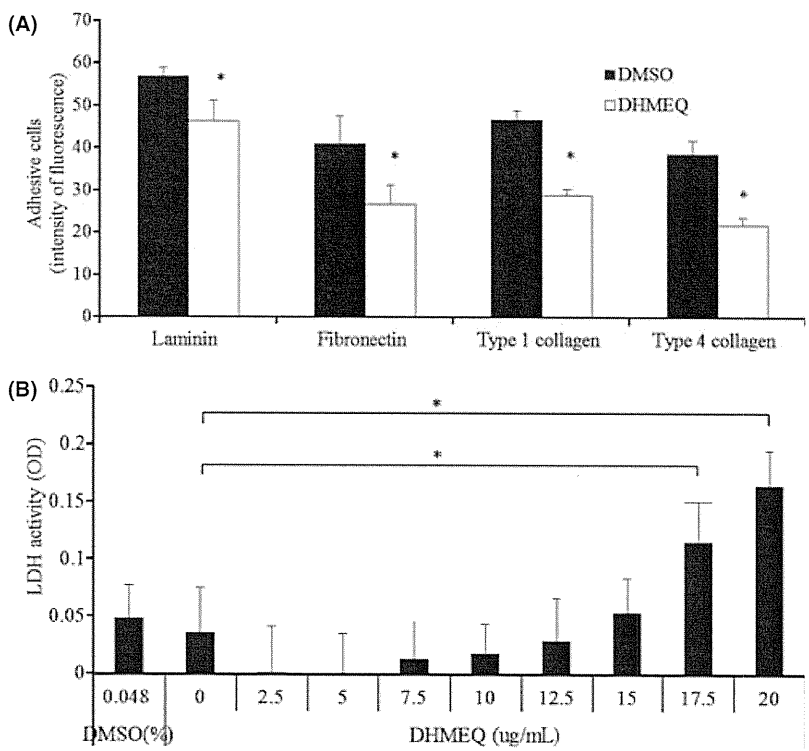

Fig. 3. Anti-adhesive effect of dehydroxymethylepoxyquinomicin (DHMEQ) pretreated cells in the *in vitro* study. (A) Adhesion assay. The bars show the fluorescence intensity of the remaining live cells on the plates. The black bars show cells pretreated with DHMEQ, and white bars show those with DMSO. *Significantly less than controls ($P < 0.05$). (B) Evaluation of cytotoxicity of DHMEQ. The graph shows lactate dehydrogenase (LDH) activity of the supernatant of the 44As3Luc cells treated with DHMEQ or DMSO. *$P < 0.05$. OD, optical density.

peritoneal lavage (Fig. 4B). The SEM revealed that cancer cells adhered less to the basement membrane of the peritoneum in mice injected with DHMEQ-pretreated cells than in those injected with DMSO-pretreated control cells (Fig. 4C).

Follow up of gastric cancer dissemination by *in vivo* imaging. The DHMEQ-pretreated 44As3Luc cells injected in mice grew slowly compared with the DMSO-pretreated cells (Fig. 5A). The increase in the CPM/mm^2 value of the

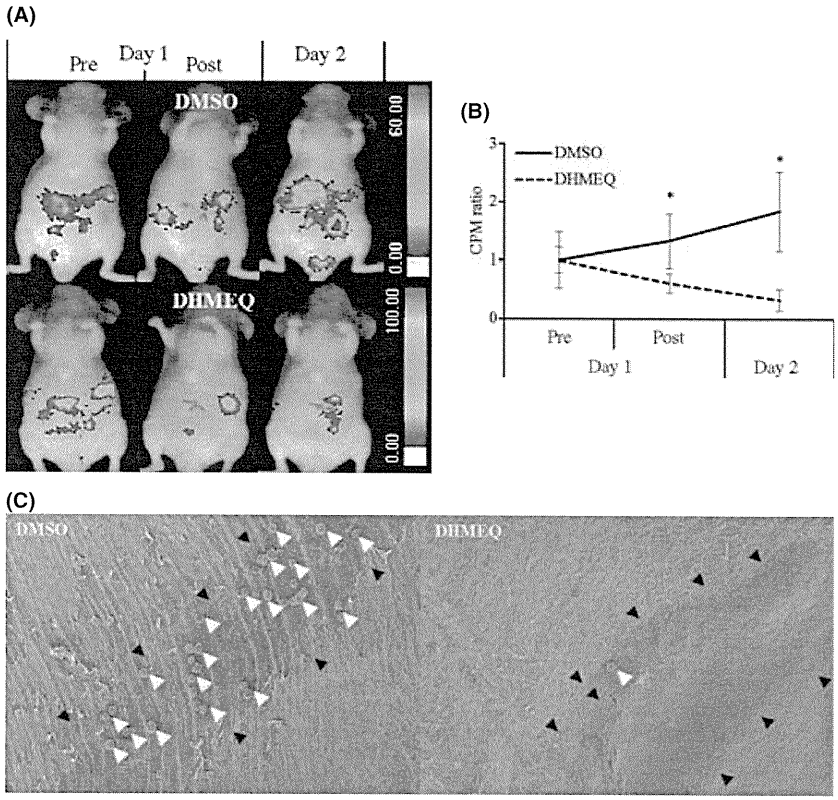

Fig. 4. Peritoneal lavage inhibited cancer cells pretreated with dehydroxymethylepoxyquinomicin (DHMEQ) from implanting into the abdominal wall. (A) *In vivo* imaging at around the time of peritoneal lavage. The luminescent value indicates the number of live cells in the abdominal wall. Pre/Post means before/after the peritoneal lavage. (B) Count per minute (CPM)/mm^2 value of pre/post peritoneal lavage. The graph shows the time course of the CPM/mm^2 value compared with the time of cancer cell injection. Initial values were adjusted to 1. *Significantly less than controls ($P < 0.05$). (C) SEM findings of the peritoneum. Left: abdominal wall injected with 44As3Luc cells pretreated with DHMEQ. Right: those with DMSO. The area indicated by black arrowheads is the area exposed to the peritoneal cavity. White arrowheads show the adhesive cancer cells.

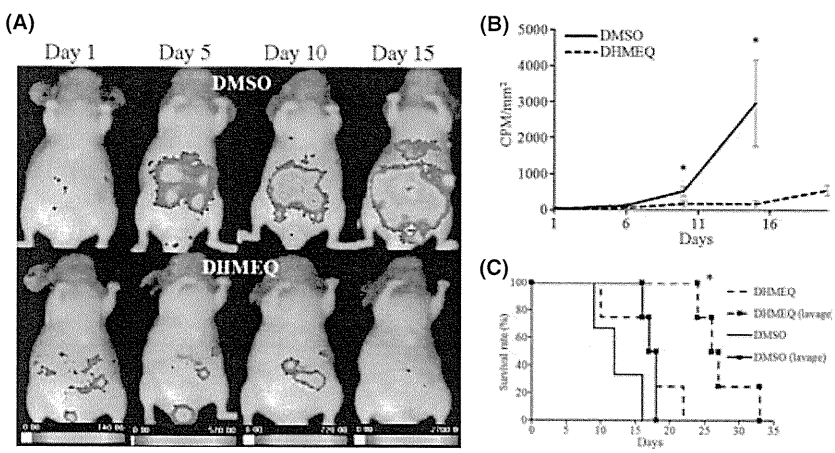

Fig. 5. Follow up after peritoneal lavage. (A) Follow-up imaging of mice subjected to peritoneal lavage. The range bars were adjusted for mice injected with DMSO pretreated cells at every evaluation day. (B) Time course of the count per minute (CPM)/mm^2 value. The black line represents the mice that were injected with DMSO-pretreated cells, and the broken line represents those injected with dehydroxymethylepoxyquinomicin (DHMEQ)-pretreated cells. *Significantly less than controls ($P < 0.05$). (C) Kaplan–Meier analysis of the survival of all groups. The line is as described above. The line with markers represents mice subjected to peritoneal lavage. *Significantly prolonged than all other groups ($P < 0.05$).

DHMEQ-treated cells was significantly delayed. The error bar of the CPM/mm^2 value of the DMSO-pretreated group ranged widely, because malignant ascites possibly obscured luminescent emission at the terminal stage (Fig. 5B). Survival was only significantly prolonged in mice injected with DHMEQ-treated cells and subjected to peritoneal lavage (Fig. 5C).

Discussion

NF-κB is undoubtedly involved in various biological properties of cancer cells.[35] However, its involvement in the expression of integrins, which are associated with cancer cell adhesion to the peritoneum, has not been reported. In the present study, we investigated whether NF-κB is involved in cell adhesion to the peritoneum via regulation of integrin expression, and whether DHMEQ, as a novel NF-κB inhibitor, suppresses the dissemination of gastric cancer in a mouse model.

Several investigators reported that NF-κB activity is associated with peritoneal dissemination of cancer cells.[36–38] Sasaki *et al.*[39] evaluated human gastric cancer tissues by immunohistochemical analysis, where NF-κB activation was significantly correlated with peritoneal metastases and survival. Our results in the present study support the previously reported data that NF-κB activity of gastric cancer cell lines was markedly activated and with highly metastatic behavior, and that DHMEQ sufficiently inhibited NF-κB activity and eventually suppressed the peritoneal dissemination.

Integrins are also associated with malignant potential.[40–42] Integrins play an important role in cancer cell adhesion to the peritoneum by enabling contact with appropriate ECM. Oosterling *et al.*[43] showed that anti-β1 integrin antibody reduces surgery-induced adhesion of colon carcinoma cells to traumatized peritoneal surfaces. Fishman *et al.*[44] showed similar findings using ovarian cancer cell lines in the *in vitro* analysis. With

doi: 10.1111/j.1349-7006.2011.01901.x

regard to gastric cancer, integrins α2, α3 and β1 are key molecules in animal models and humans.[11,12,45,46] The ligands of integrin α2β1 are collagens and laminin, and those of α3β1 are fibronectin, laminin,and collagens.[10] In our *in vitro* study, DHMEQ suppressed cancer cell adhesion to the peritoneum via p65-mediated suppression of integrin expression. Also, Takatsuki *et al.*[12] reported that anti-α3 antibody strongly suppressed the adhesion of gastric cancer cells to mice peritoneum. This integrin α3 was suppressed most by DHMEQ in this study. Therefore, DHMEQ may suppress cancer cell adhesion mainly via integrin α3, while DHMEQ may associate with other adhesion molecules that are not examined in this study.

In our *in vivo* study, viable cells in mice injected with DHMEQ-treated cells and subjected to peritoneal lavage still decreased on day 2 and only this group survived significantly longer. This finding might suggest that DHMEQ exerts another effect via the anti-adhesive effect. Jiang *et al.*[47] reported that NF-κB inhibition by IκBβ reduces anchorage-independent growth in a lung cancer cell line. Scaife *et al.*[48] showed that NF-κB inhibitor causes anoikis in a human colon cancer cell line. It might be possible that DHMEQ is associated with a pro-anoikis effect in gastric cancer dissemination.

In the present study, we first demonstrated that NF-κB could play a pivotal role in the progression of gastric cancer via the regulation of integrin expression and promotion of adhesion of cancer cells to the peritoneal wall. In our *in vivo* study, a specific deletion of NF-κB (p65) by siRNA was not performed, because we considered that transient deletion of p65 protein does not reflect the same result of DHMEQ-administered cells. Additionally, we could not clarify whether the DHMEQ effect on integrins is unique to the integrin pathway or concomitant with other phenomenon such as apoptosis. Further studies are required to clarify the involvement of integrins or other molecules in the anti-adhesive effect of DHMEQ against cancer cells. We believe that NF-κB inhibitors such as DHMEQ may be potential therapeutic options to prevent gastric cancer progression during peri-operative periods.

Acknowledgments

This study were supported by the Program for Promotion of Fundamental Studies in Health Sciences of the National Institute of Biomedical Innovation (NIBIO) and by a Grant-in-Aid for Scientific Research from the Ministry of Education, Culture, Sports, Science and Technology of Japan (#17390357 and #19659317 to M.O., # 21390369 to T.K.). We also thank Dr M. Takigahira (Section for Studies on Metastasis, National Cancer Center Research Institute, Chuo-ku, Tokyo, Japan) for her excellent technical support for constructing the 44As3Luc cells, Ms N. Kobayashi (Department of General Surgery, Graduate School of Medicine, Hokkaido University, Sapporo, Japan) for performing the real-time PCR assay and Dr H. Maeda (Creative Research Institution, Hokkaido University, Sapporo, Japan) for processing the samples for SEM.

Disclosure Statement

The authors have no conflict of interest.

References

1 Sasako M. Principles of surgical treatment for curable gastric cancer. *J Clin Oncol* 2003; **21**: 274s–5s.
2 Schott A, Vogel I, Krueger U *et al.* Isolated tumor cells are frequently detectable in the peritoneal cavity of gastric and colorectal cancer patients and serve as a new prognostic marker. *Ann Surg* 1998; **227**: 372–9.
3 Sadeghi B, Arvieux C, Glehen O *et al.* Peritoneal carcinomatosis from non-gynecologic malignancies: results of the EVOCAPE 1 multicentric prospective study. *Cancer* 2000; **88**: 358–63.
4 Kimura A, Koga S, Kudoh H, Iitsuka Y. Peritoneal mesothelial cell injury factors in rat cancerous ascites. *Cancer Res* 1985; **45**: 4330–3.
5 Yonemura Y, Endo Y, Obata T, Sasaki T. Recent advances in the treatment of peritoneal dissemination of gastrointestinal cancers by nucleoside antimetabolites. *Cancer Sci* 2007; **98**: 11–8.
6 Witz CA, Montoya-Rodriguez IA, Cho S, Centonze VE, Bonewald LF, Schenken RS. Composition of the extracellular matrix of the peritoneum. *J Soc Gynecol Investig* 2001; **8**: 299–304.
7 Lessan K, Aguiar DJ, Oegema T, Siebenson L, Skubitz AP. CD44 and beta1 integrin mediate ovarian carcinoma cell adhesion to peritoneal mesothelial cells. *Am J Pathol* 1999; **154**: 1525–37.
8 Ruoslahti E, Giancotti FG. Integrins and tumor cell dissemination. *Cancer Cells* 1989; **1**: 119–26.
9 Hehlgans S, Haase M, Cordes N. Signalling via integrins: implications for cell survival and anticancer strategies. *Biochim Biophys Acta* 2007; **1775**: 163–80.
10 Hynes RO. Integrins: versatility, modulation, and signaling in cell adhesion. *Cell* 1992; **69**: 11–25.
11 Nishimura S, Chung YS, Yashiro M, Inoue T, Sowa M. Role of alpha 2 beta 1- and alpha 3 beta 1-integrin in the peritoneal implantation of scirrhous gastric carcinoma. *Br J Cancer* 1996; **74**: 1406–12.
12 Takatsuki H, Komatsu S, Sano R, Takada Y, Tsuji T. Adhesion of gastric carcinoma cells to peritoneum mediated by alpha3beta1 integrin (VLA-3). *Cancer Res* 2004; **64**: 6065–70.
13 Sen R, Baltimore D. Multiple nuclear factors interact with the immunoglobulin enhancer sequences. *Cell* 1986; **46**: 705–16.
14 Berkholtz CB, Lai BE, Woodruff TK, Shea LD. Distribution of extracellular matrix proteins type I collagen, type IV collagen, fibronectin, and laminin in mouse folliculogenesis. *Histochem Cell Biol* 2006; **126**: 583–92.
15 Verma IM, Stevenson JK, Schwarz EM, Van Antwerp D, Miyamoto S. Rel/NF-kappa B/I kappa B family: intimate tales of association and dissociation. *Genes Dev* 1995; **9**: 2723–35.
16 Donnellan R, Chetty R. Cyclin D1 and human neoplasia. *Mol Pathol* 1998; **51**: 1–7.
17 Bonizzi G, Karin M. The two NF-kappaB activation pathways and their role in innate and adaptive immunity. *Trends Immunol* 2004; **25**: 280–8.
18 Karin M, Cao Y, Greten FR, Li ZW. NF-kappaB in cancer: from innocent bystander to major culprit. *Nat Rev Cancer* 2002; **2**: 301–10.
19 Deveraux QL, Reed JC. IAP family proteins – suppressors of apoptosis. *Genes Dev* 1999; **13**: 239–52.
20 Tergaonkar V, Pando M, Vafa O, Wahl G, Verma I. p53 stabilization is decreased upon NFkappaB activation: a role for NFkappaB in acquisition of resistance to chemotherapy. *Cancer Cell* 2002; **1**: 493–503.
21 Huang S, Robinson JB, Deguzman A, Bucana CD, Fidler IJ. Blockade of nuclear factor-kappaB signaling inhibits angiogenesis and tumorigenicity of human ovarian cancer cells by suppressing expression of vascular endothelial growth factor and interleukin 8. *Cancer Res* 2000; **60**: 5334–9.
22 Rangaswami H, Bulbule A, Kundu GC. Nuclear factor-inducing kinase plays a crucial role in osteopontin-induced MAPK/IkappaBalpha kinase-dependent nuclear factor kappaB-mediated promatrix metalloproteinase-9 activation. *J Biol Chem* 2004; **279**: 38921–35.
23 Bentires-Alj M, Barbu V, Fillet M *et al.* NF-kappaB transcription factor induces drug resistance through MDR1 expression in cancer cells. *Oncogene* 2003; **22**: 90–7.
24 Ariga A, Namekawa J, Matsumoto N, Inoue J, Umezawa K. Inhibition of tumor necrosis factor-alpha-induced nuclear translocation and activation of NF-kappa B by dehydroxymethylepoxyquinomicin. *J Biol Chem* 2002; **277**: 24625–30.
25 Yamamoto M, Horie R, Takeiri M, Kozawa I, Umezawa K. Inactivation of NF-kappaB Components by Covalent Binding of (−)-Dehydroxymethylepoxyquinomicin to Specific Cysteine Residues. *J Med Chem* 2008; **51**: 5780–8.
26 Watanabe M, Ohsugi T, Shoda M *et al.* Dual targeting of transformed and untransformed HTLV-1-infected T cells by DHMEQ, a potent and selective inhibitor of NF-kappaB, as a strategy for chemoprevention and therapy of adult T-cell leukemia. *Blood* 2005; **106**: 2462–71.
27 Starenki DV, Namba H, Saenko VA *et al.* Induction of thyroid cancer cell apoptosis by a novel nuclear factor kappaB inhibitor, dehydroxymethylepoxyquinomicin. *Clin Cancer Res* 2004; **10**: 6821–9.
28 Tatetsu H, Okuno Y, Nakamura M *et al.* Dehydroxymethylepoxyquinomicin, a novel nuclear factor-kappaB inhibitor, induces apoptosis in multiple myeloma cells in an IkappaBalpha-independent manner. *Mol Cancer Ther* 2005; **4**: 1114–20.
29 Kikuchi E, Horiguchi Y, Nakashima J *et al.* Suppression of hormone-refractory prostate cancer by a novel nuclear factor kappaB inhibitor in nude mice. *Cancer Res* 2003; **63**: 107–10.
30 Nishimura D, Ishikawa H, Matsumoto K *et al.* DHMEQ, a novel NF-kappaB inhibitor, induces apoptosis and cell-cycle arrest in human hepatoma cells. *Int J Oncol* 2006; **29**: 713–9.

31 Matsumoto G, Namekawa J, Muta M *et al.* Targeting of nuclear factor kappaB Pathways by dehydroxymethylepoxyquinomicin, a novel inhibitor of breast carcinomas: antitumor and antiangiogenic potential in vivo. *Clin Cancer Res* 2005; **11**: 1287–93.
32 Matsumoto G, Muta M, Umezawa K *et al.* Enhancement of the caspase-independent apoptotic sensitivity of pancreatic cancer cells by DHMEQ, an NF-kappaB inhibitor. *Int J Oncol* 2005; **27**: 1247–55.
33 Dabaghmanesh N, Matsubara A, Miyake A *et al.* Transient inhibition of NF-kappaB by DHMEQ induces cell death of primary effusion lymphoma without HHV-8 reactivation. *Cancer Sci* 2009; **100**: 737–46.
34 Yanagihara K, Takigahira M, Takeshita F *et al.* A photon counting technique for quantitatively evaluating progression of peritoneal tumor dissemination. *Cancer Res* 2006; **66**: 7532–9.
35 Nakanishi C, Toi M. Nuclear factor-kappaB inhibitors as sensitizers to anticancer drugs. *Nat Rev Cancer* 2005; **5**: 297–309.
36 Mabuchi S, Ohmichi M, Nishio Y *et al.* Inhibition of inhibitor of nuclear factor-kappaB phosphorylation increases the efficacy of paclitaxel in in vitro and in vivo ovarian cancer models. *Clin Cancer Res* 2004; **10**: 7645–54.
37 Nakahara C, Nakamura K, Yamanaka N *et al.* Cyclosporin-A enhances docetaxel-induced apoptosis through inhibition of nuclear factor-kappaB activation in human gastric carcinoma cells. *Clin Cancer Res* 2003; **9**: 5409–16.
38 Shao M, Cao L, Shen C *et al.* Epithelial-to-mesenchymal transition and ovarian tumor progression induced by tissue transglutaminase. *Cancer Res* 2009; **69**: 9192–201.
39 Sasaki N, Morisaki T, Hashizume K *et al.* Nuclear factor-kappaB p65 (RelA) transcription factor is constitutively activated in human gastric carcinoma tissue. *Clin Cancer Res* 2001; **7**: 4136–42.
40 Pontes-Junior J, Reis ST, de Oliveira LC *et al.* Association between integrin expression and prognosis in localized prostate cancer. *Prostate* 2010; **70**: 1189–95.
41 Dingemans AM, van den Boogaart V, Vosse BA, van Suylen RJ, Griffioen AW, Thijssen VL. Integrin expression profiling identifies integrin alpha5 and beta1 as prognostic factors in early stage non-small cell lung cancer. *Mol Cancer* 2010; **9**: 152.
42 Takayama N, Arima S, Haraoka S, Kotho T, Futami K, Iwashita A. Relationship between the expression of adhesion molecules in primary esophageal squamous cell carcinoma and metastatic lymph nodes. *Anticancer Res* 2003; **23**: 4435–42.
43 Oosterling SJ, van der Bij GJ, Bogels M *et al.* Anti-beta1 integrin antibody reduces surgery-induced adhesion of colon carcinoma cells to traumatized peritoneal surfaces. *Ann Surg* 2008; **247**: 85–94.
44 Fishman DA, Kearns A, Chilukuri K *et al.* Metastatic dissemination of human ovarian epithelial carcinoma is promoted by alpha2beta1-integrin-mediated interaction with type I collagen. *Invasion Metastasis* 1998; **18**: 15–26.
45 Kawamura T, Endo Y, Yonemura Y *et al.* Significance of integrin alpha2/beta1 in peritoneal dissemination of a human gastric cancer xenograft model. *Int J Oncol* 2001; **18**: 809–15.
46 Matsuoka T, Yashiro M, Nishimura S *et al.* Increased expression of alpha2beta1-integrin in the peritoneal dissemination of human gastric carcinoma. *Int J Mol Med* 2000; **5**: 21–5.
47 Jiang Y, Cui L, Yie TA, Rom WN, Cheng H, Tchou-Wong KM. Inhibition of anchorage-independent growth and lung metastasis of A549 lung carcinoma cells by IkappaBbeta. *Oncogene* 2001; **20**: 2254–63.
48 Scaife CL, Kuang J, Wills JC *et al.* Nuclear factor kappaB inhibitors induce adhesion-dependent colon cancer apoptosis: implications for metastasis. *Cancer Res* 2002; **62**: 6870–8.

doi: 10.1111/j.1349-7006.2011.01901.x

Molecular Vision 2012; 18:455-464 <http://www.molvis.org/molvis/v18/a49>
Received 8 January 2012 | Accepted 10 February 2012 | Published 14 February 2012

Amelioration of ultraviolet-induced photokeratitis in mice treated with astaxanthin eye drops

Anton Lennikov,[1] Nobuyoshi Kitaichi,[1,2,3] Risa Fukase,[1] Miyuki Murata,[1,2] Kousuke Noda,[1] Ryo Ando,[1] Takeshi Ohguchi,[1] Tetsuya Kawakita,[4] Shigeaki Ohno,[2] Susumu Ishida[1]

[1]Laboratory of Ocular Cell Biology and Visual Science, Department of Ophthalmology, Hokkaido University Graduate School of Medicine, Sapporo, Japan; [2]Department of Ocular Inflammation and Immunology, Hokkaido University Graduate School of Medicine, Sapporo, Japan; [3]Department of Ophthalmology, Health Sciences University of Hokkaido, Sapporo, Japan; [4]Department of Ophthalmology, Keio University, School of Medicine, Tokyo, Japan

Purpose: Ultraviolet (UV) acts as low-dose ionizing radiation. Acute UVB exposure causes photokeratitis and induces apoptosis in corneal cells. Astaxanthin (AST) is a carotenoid, present in seafood, that has potential clinical applications due to its high antioxidant activity. In the present study, we examined whether topical administration of AST has preventive and therapeutic effects on UV-photokeratitis in mice.

Methods: C57BL/6 mice were administered with AST diluted in polyethylene glycol (PEG) in instillation form (15 µl) to the right eye. Left eyes were given vehicle alone as controls. Immediately after the instillation, the mice, under anesthesia, were irradiated with UVB at a dose of 400 mJ/cm^2. Eyeballs were collected 24 h after irradiation and stained with H&E and TUNEL. In an in vitro study, mouse corneal epithelial (TKE2) cells were cultured with AST before UV exposure to quantify the UV-derived cytotoxicity.

Results: UVB exposure induced cell death and thinning of the corneal epithelium. However, the epithelium was morphologically well preserved after irradiation in AST-treated corneas. Irradiated corneal epithelium was significantly thicker in eyes treated with AST eye drops, compared to those treated with vehicles ($p<0.01$), in a doses dependent manner. Significantly fewer apoptotic cells were observed in AST-treated eyes than controls after irradiation ($p<0.01$). AST also reduced oxidative stress in irradiated corneas. The in vitro study showed less cytotoxicity of TKE2 cells in AST-treated cultures after UVB-irradiation ($p<0.01$). The cytoprotective effect increased with the dose of AST.

Conclusions: Topical AST administration may be a candidate treatment to limit the damages by UV irradiation with wide clinical applications.

Ultraviolet (UV) irradiation represents a significant environmental hazard that can cause acute and chronic inflammatory changes in the cornea, lens, and retina of the eye. The sources of UV radiation are not merely from electric welding and tanning lamps but also from sunny days on the sea or in snowy mountains when eyes are left unprotected. In recent decades, the risk of acute photochemically-induced ocular damage has increased due to stratospheric ozone depletion [1]. UVB exposure causes photokeratitis, which is associated with expression of nuclear factor (NF)-κB, prostaglandin E2 (PGE2), and many other inflammatory agents [1]. Acute UVB exposure causes damage deeper than the epithelium, involving all tissues of the cornea [2] and inducing apoptosis in corneal cells [3,4]. Although the energy is much less than that of the gamma rays, ophthalmologists find it is necessary to study ways to prevent the damages caused by UV radiation due to its association with clinical ocular diseases. We have already reported that applying UVB irradiation at 400 mJ/cm^2 to mice corneas can be a useful model for studying corneal inflammation [3].

Antioxidant enzymes, such as superoxide dismutase [5] and catalase [6], and pharmacologic antioxidants like N-acetyl cysteine [7,8], inhibit tumor necrosis factor (TNF)-α activation through NF-κB-dependent gene expression [9]. Astaxanthin (AST), 3,30-dihydroxy-b,b-carotene-4,40-dione, a carotenoid without vitamin A activity [10,11], has potential clinical applications due to its antioxidant activity, which is higher than β-carotene and α-tocopherol [10,12,13]. In addition, it has many highly potent pharmacological effects, including anti-tumor, anti-cancer, anti-diabetic, and anti-inflammation activities [12,14-16]. The potent activity of AST has been observed to modulate biologic functions ranging from lipid peroxidation to tissue protection [14,17]. The presence of the hydroxyl (OH) and keto (C=O) on each ionone ring in AST explains its unique feature of antioxidant activity for the protection of both the inner and outer membrane surfaces [10,14,18,19]. AST is found abundantly in the red-orange pigment of marine animals such as salmon (and salmon roe) and the shell of crabs and shrimp. AST and AST-like products are commonly indicated as

Correspondence to: Nobuyoshi Kitaichi, M.D., Ph.D., Department of Ocular Inflammation and Immunology, Hokkaido University Graduate School of Medicine, Kita-15, Nishi-7, Kita-ku, Sapporo 060-8638, Japan; Phone: +81-11-706-5944; FAX: +81-11-706-5948; email: nobukita@med.hokudai.ac.jp

antioxidants [20] and immune modulators [21]. One of the effects of AST is to scavenge reactive oxygen species [22]. We previously reported that AST showed a dose-dependent anti-inflammatory effect [23,24]. It was also reported that AST inhibited the production of inflammatory mediators by blocking NF-κB activation in vitro [4]. In the present study, we examined whether topical administration of AST has therapeutic effects on UV photokeratitis in mice.

METHODS

Animals and reagents: Six- to 8-week-old C57BL/6 male mice were obtained from Clear Japan (Tokyo, Japan). Mice were maintained under specific pathogen-free conditions. All procedures involving animals were performed in accordance with the ARVO resolution on the use of animals in research. AST was purchased from Sigma-Aldrich (Tokyo, Japan).

UV irradiation: The mice were administered with AST diluted in polyethylene glycol (PEG) in instillation form (15 µl) to the right eye once at the following concentrations: 1, 0.1, and 0.01 mg/ml (10 mice per group. Left eyes were instilled with vehicle alone. Immediately after the instillation, anesthetized mice were irradiated with UVB at a dose of 400 mJ/cm^2 from a FS-20 (Panasonic, Osaka, Japan) fluorescent lamp. These bulbs have a broad emission spectrum (250–400 nm) with high output primarily in the UVB spectrum (290–320 nm). To evaluate the effects of AST on the corneal surface without UVB damage, control mice received the instillation of 1 mg/ml of AST without irradiation. All experiments were performed in triplicate.

H&E and TUNEL staining: The eyes were dissected from mice 24 h after UVB exposure and fixed with 4% paraformalin. Tissue sections were prepared and stained with hematoxylin-eosin (H&E) for morphological analysis. Other sections were stained by terminal deoxynucleotidyl transferase dUTP nick end labeling (TUNEL) assay to detect apoptotic signaling. Apoptotic cells were detected with a Cell Death Detection Kit (Roche Diagnostics Japan, Tokyo) containing all necessary reagents for staining. Slides imaging, cell counting, and thickness evaluations were performed with BZ-9000 fluorescence microscope (Keyence, Japan) and software bundled with the apparatus. At least 10 sections were used to evaluate the epithelial thickness, measurements of 10 randomly selected areas of epithelium of central cornea was performed and averaged.

Evaluation of the "sunglasses effect" of AST: The "sunglass effect" represents the status when protective properties of a substance are only due to blocking the UV rather than having a cytoprotective effect. To evaluate this effect, and whether AST is capable of rescuing the damaged epithelia after UVB irradiation, we performed additional experiments where mice were first irradiated with UVB at a dose of 400 mJ/cm^2 under anesthesia. After 5 min of irradiation, the right eyes were then instilled with AST (1 mg/ml) and the left eyes instilled with vehicle alone.

Detection of reactive oxygen species (ROS): The eyes were dissected from mice 24 h after UVB exposure and frozen fresh in optimal cutting temperature (OCT) compound with liquid nitrogen. To visualize not only oxidative signaling but also the tissue structure, 4',6-diamidino-2-phenylindole (DAPI) dye (blue) was used to stain the nuclei of the cells. Dihydroethidium (DHE; Sigma-Aldrich, St. Louis, MO), an oxidative fluorescent dye, was used for the immunohistochemical detection of cytosolic superoxide anion (O_2^-) to evaluate ROS production in corneal epithelium tissue, as reported recently [25].

NF-κB immunohistochemistry staining: The eyes were dissected from mice 24 h after UVB exposure and fixed with 4% paraformaldehyde and then paraffin-embedded. To evaluate the NF-κB positive cells in the corneal epithelium, slides were rehydrated and applied with a 1:50 dilution of NF-κB P65 antibody (Santa Cruz Biotechnology, Santa Cruz, CA) for 12 h, washed with PBS and then applied with 1:100 dilution of secondary goat anti–rabbit antibody dye conjugate (Invitrogen, Carlsbad, CA), which gives red fluorescence. Since NF-κB is widely present in intercellular tissue, to detect its expression in cell nuclei, we stained the section slides with 1:100 dilution of YO-PRO®-1 (Invitrogen), which produces a green signal from the cell nuclei. NF-κB positive (yellow) nuclei were quantified in merged images.

In vitro study: TKE2 cells were used for in vitro study. TKE2 is a murine corneal epithelium-derived progenitor cell line [26,27]. Mouse TKE2 cells were cultured in Defined K-SFM (Keratinocye Serum Free Medium) with L-Glutamine, Phenol Red, and Sodium Pyruvate (Invitrogen), supplemented with 100 U/ml of penicillin and 100 U/ml of streptomycin, (Invitrogen). The cells were seeded onto 24-well plates (5×10^4 cells/well) at 37 °C in a humidified incubator containing 5% CO_2. The cells were treated with 1, 0.1, or 0.01 mg/ml AST. After 6 h of incubation, the wells were irradiated with UVB at a dose of 300 mJ/cm^2 at room temperature for 1 min. To prevent UVB radiation absorption, the culture media were removed just before irradiation and replaced with a thin layer of phosphate-buffered saline (PBS). After UVB irradiation, cells were fed with fresh medium. The LDH (lactate dehydrogenase) Cytotoxicity Detection Kit (Roche Applied Science, Penzberg, Germany) was used to determine cytotoxicity 6 h after UVB exposure. Culture supernatants (100 µl) were collected and added to the kit's work solution. After 30 min incubation, the absorbance was measured with an ELISA reader. All procedures were performed according the user manual of the kit. Analysis was performed in triplicate. To determine the background LDH activity of the medium and spontaneous LDH release, additional plates were prepared with empty medium and unaffected cells. The maximum LDH release was achieved by adding 100 µl of Triton-B to the reference wells. Cytotoxicity percentages were calculated, and Triton-B treated wells with

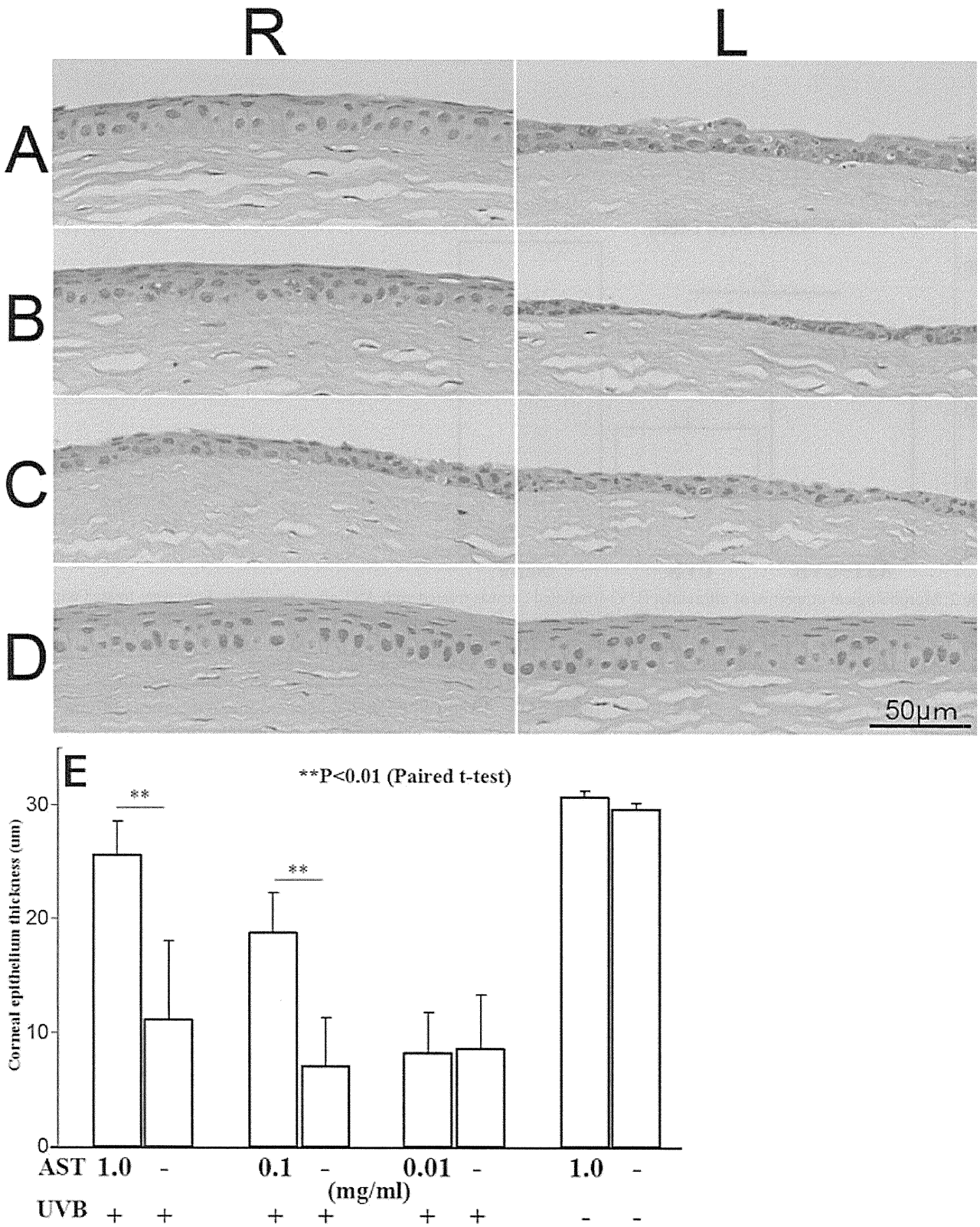

Figure 1. Morphological properties of ultraviolet (UV)-irradiated corneas. Eyes were treated with AST eye drops before UV exposure (**A**: 1 mg/ml, **B**: 0.1 mg/ml, **C**: 0.01 mg/ml AST). Control subjects were not irradiated with UVB (**D**). R: Right eyes were given various concentrations of AST eye drops. L: Left eyes were given vehicle alone as controls. The mean values of corneal epithelial thickness are summarized (E). Epithelia were significantly thicker in right eyes treated with 1 and 0.1 mg/ml AST compared to the left eyes, which served as controls ($p<0.01$). Protective effects of AST were found to occur in a dose-dependent manner.